ADDIS ABABA UNIVERSITY

ADDIS ABABA INSTITUTE OF TECHNOLOGY

School of Mechanical and Industrial Engineering

Experimental investigation and optimization of Wear property of Al-TiB_2-Gr hybrid composite

A Thesis submitted to the School of Mechanical and Industrial Engineering of Addis Ababa University in partial fulfillment of the Degree of Master of Science

In

Mechanical Engineering (Manufacturing stream)

By: Daniel Mekasha GSR/1584/14
Advisor: Dr. Desalegn Wogaso

June, 2024

DECLARATION

I hereby declare that this thesis research: "**Experimental investigation and optimization of Wear property of Al-TiB_2-Gr hybrid composite**" is my own work and this work has not been submitted elsewhere for the award of any other degree or diploma. It is being submitted for the degree of Master of Science in Mechanical Engineering (Manufacturing Engineering), and all sources of material used for this thesis have been duly acknowledged.

Daniel Mekasha		
Student Name	Signature	Date

This thesis research has been submitted for examination with approval as a thesis advisor.

Dr. Desalegn Wogaso		
Advisor	Signature	Date

Addis Ababa University

Addis Ababa Institute of Technology

School of Mechanical and Industrial Engineering

Experimental investigation and optimization of Wear property of Al-TiB_2-Gr hybrid composite

By: DANIEL MEKASHA

Submitted by the requirement or the degree of

Masters of Science (M.Sc.)

Approved by Board of Examiners:

Dr. Desalegn Wogaso	____________	____________
Advisor	Signature	Date
Dr. Mesfin Gizaw	____________	____________
Internal Examiner	Signature	Date
Mr Henok Zewdu (PhD Candidate)	____________	____________
External Examiner	Signature	Date
Dr. Araya Abera	____________	____________
Dean, School of Mechanical and Industrial Engineering	Signature	Date
Dr. Sosina Mengistu	____________	____________
Associate Director of Postgraduate Program	Signature	Date

ACKNOWLEDGEMENT

I sincerely would like to offer my deepest gratitude to my advisor Dr. Desalegn Wogaso for his invaluable patience, continuous follow-up and feedback, and constructive criticism from the start of this paperwork. And also, his hard-working habit motivates me to be more ambitious for further work. I also could not have undertaken this journey without a lot of good friends and professionals that I knew from working with them during this study. Just to name a few, Mr. Mekonen, Mr. Mengistu, and Mr. Lata from Adama Science and Technology University have been a very big help to me. I am also grateful to Mr. Yemane who has been very helpful and patient, working tirelessly even on his lunch breaks and always giving me his time from his busy schedule. Additionally, this endeavor would not have been possible without the help from the School of Mechanical and Industrial Engineering in AAiT for providing access to the available utilities. A big thanks should also go to the shop supervisors, Lab assistants, and others from the university, who impacted and helped me, and all the people who lent me their hands whenever needed, until the end of this study.

Lastly, I would be remiss in not mentioning my family and friends. Their belief in me and emotional support have kept my spirits and motivation high during this process. Words cannot express my gratitude to all of them. Thank you!

ABSTRACT

In recent days, monolithic metals and conventional alloys are being replaced by aluminum metal matrix composites in many applications in the field of automotive and aerospace due to a high strength-to-weight ratio, fracture limit, toughness, wear, and sustaining properties at higher temperatures. This investigation thus deals with the fabrication of aluminum metal matrix hybrid composites by stir casting technique with reinforcement of TiB_2 and Gr in varying percentages through the stir casting process. Reinforcements are added in 10% TiB_2 and 0%, 2%, 4%, 6%, and 8% in volume percentage of graphite particulate into Al 6061 for composite preparation. The wear and hardness properties of the hybrid composite material were studied and a microstructural examination was presented. The wear performance of the specimens was measured using the pin-on-disc technique and optimization of process parameters was conducted according to the DOE and optimized by Taguchi analysis.

The results showed that the reinforcements twinned and measuring only a few µm in size, were embedded in the aluminum matrix, having an equiaxed grain structure. By the addition of 2% of graphite reinforcement, the microhardness value was drastically improved by 45.6%, from 23.2 to 33.8HV. From Sample 2 to Sample 6, the hardness increased gradually. The Maximum hardness value for this experiment, 43.43HV, was obtained in 10% reinforcement composition to give a total of 86.59% improvement in hardness. The COF from the pin-on-disk test also showed a 20.52% decrement, from 0.54 to 0.38um, at 10% composition of Gr particle because of its lubricating characteristics. The wear rate of composites reinforced with 8% graphite and 10% graphite declined by 83.18% and 85.77%, respectively, showing that the wear rate also decreases as graphite composition increases. The optimum parametric condition for COF and wear rate was achieved when the combination of factors is at a Load of 30N, at a Speed of 200RPM, and for 10 minutes with confirmation of test also supporting the conclusion with a 10.11% and 7.37%, respectively, deviation from the predicted value.

Key Words: *Hybrid Composite, Graphite, Wear Property, Wear Parameters, Stir Casting, Titanium Diboride, MMCs, Al-6061, Taguchi*

LIST OF ACRONYMS AND ABBREVIATIONS

AAIT	**Addis Ababa Institute of Technology**
AASTU	**Addis Ababa Science and Technology University**
ANOVA	**Analysis of Variance**
ASTM	**American Society for Testing and Materials**
CNT	**Carbon nano-tubes**
GNP	**Graphene-nanoplatelets**
FEA	**Finite Element Analysis**
FEGV	**Fan Exit Guide Vanes**
LVDT	**Linear Variable Differential Transformer**
MMC	**Metal Matrix Composite**
SEM	**Scanning Electron Microscope**
UTS	**Ultimate Tensile Strength**
WT%	**Weight Percentage**
OA	**Orthogonal Array**

TABLE OF CONTENTS

LIST OF TABLES

LIST OF FIGURES

CHAPTER ONE

1. INTRODUCTION

1.1. BACKGROUND OF THE STUDY

Composite material plays a greater part in all types of applications because researchers are unremittingly trying to find new materials to meet their requirements with different materials and production methods [1]. The development of aluminum matrix composites (AMCs), a particular type of composite material, has been fueled by the growing needs of the transportation, agricultural, construction, and manufacturing industries for lightweight materials, that have a high specific strength, perform exceptionally well at high temperatures, are chemically inert, and require less energy. In many cutting-edge applications, these materials which are lightweight and highly effective have the potential to replace traditional materials.[2].

Stir-casting is widely used among researchers due to its cost-effectiveness, fewer particle damage, and maximum metal yield range. Compared to many ceramic-strengthening particles, titanium diboride (TiB_2) particles are much more stiff, rigid, and have a greater thermal stability range [3].

Most of the commercial work on MMCs has focused on aluminum as the matrix metal. The combination of lightweight, environmental resistance, and useful mechanical properties has made aluminum alloys very popular; these properties also make aluminum well-suited for use as a matrix metal [4]. Currently, many methods are used to make different classes of AMCs. Numerous new scientific insights on the inherent and extrinsic impacts of ceramic reinforcement on the mechanical, thermomechanical, tribological, and physical properties of AMCs have been gained over decades of intensive research. [4-7].

Aluminum's favorable qualities along with its special qualities contributed to its increasing appeal. Aluminum has found more uses for alloying than initially thought, positioning it as a formidable rival to the conventional "strong" metals iron and steel, and occasionally even as a preferred option. Since aluminum was first identified as a metal of industrial relevance, it was mostly used to make decorative and domestic goods. Only later did aluminum play a significant role in the building of tremendous industrial structures and machine parts. Aluminum's use was expanded with the development of alloying technology, which made it the most widely used industrial metal for many years [8].

1.2. RATIONALE OF THE STUDY

A type of materials known Metal Matrix Composites (MMCs) has the potential to be used in many different structural and thermal management applications. Metal matrix composites can operate at higher temperatures and be tailored to offer superior strength, stiffness, thermal conductivity, abrasion resistance, creep resistance, or dimensional stability when compared to their base metal equivalents. They are not combustible, do not outgas in a vacuum, and are not as attacked by organic fluids like fuels and solvents as resin-matrix composites are [4].

Aluminum plate is used mainly in the fuselage, wing skin, oil tank, and other structural components of aircraft. It is possible to reduce the outer skin density of an airplane by 5%–7% by utilizing aluminum composite materials. This leads to a 10% reduction in overall weight and an increase in fuel economy. Additionally, incorporating aluminum can boost the material's rigidity by 7%. because aluminum alloy has exceptional fatigue, corrosion, and damage tolerance [6].

It is possible for reinforcements to make up between 10 and 60 vol% of the composite. They can be continuous or discontinuous. Refractory metals, graphite, silicon carbide, boron, and aluminum oxide (Al_2O_3) are examples of continuous fiber or filament reinforcing elements. Continuous reinforcements are mostly made of graphite or Al_2O_3 short or chopped fibers, whisker forms of SiC, particulate kinds of SiC, or titanium diboride. The utilization of unidirectional lay-up in engineering constructions is allowed by some matrix-dominated composites due to their high transverse elastic modulus and strength, which are matrix-dominated mechanical properties [4].

Aluminum metal matrix composites are gaining interest as a high-tech material with a range of applications. Al MMCs have produced economic and environmental advantages in addition to notable performance-related improvements. Improved characteristics, longer component lifetimes, higher productivity, energy savings, reduced maintenance costs, and environmental advantages including less noise and airborne emissions are noteworthy among them. In many applications, these composites can take the place of monolithic materials such as polymer-based composites, ferrous alloys, and alloys made of aluminum and titanium. The entire system might be changed to gain more weight and volume reductions before being widely replaced. Ideally, Al MMCs can be seen as a way to enable significant improvements in addition to serving as a substitute for existing materials [5].

Metal matrix composites with aluminum substrates are used in various industries. In recent years, aluminum matrix composites have found widespread application in aviation. Strong, lightweight, and able to withstand high temperatures for lengthy periods in demanding conditions are requirements for the materials used in airplane construction. Aluminum composite is the suggested material for an aircraft's wings, fuselage, and support structures. Aluminum makes up the fuselage of an airplane for about 80% of its weight. Die-casting technology for aluminum is gaining importance due to its ability to create intricate shapes at lower costs and with innovative design concepts. Aluminum metal matrix composites are the preferred material due to their greater resistance to wear and corrosion, high modulus, superior specific strength and hardness, remarkable thermal properties, and decreased density [8]. Aluminum metal matrix composites are attractive materials for thermal management and have high volume reinforcement fraction. It is possible to further improve the thermal conductivity of the composite material by using high thermal conductivity reinforcements [3].

A permanent mold-cast piston, a high-pressure die-cast bicycle sprocket, an investment-cast aircraft hydraulic manifold, investment-cast engine cylinder inserts, a sand-cast automobile disk brake rotor and the upper control arm are shown in Figure 1.1.

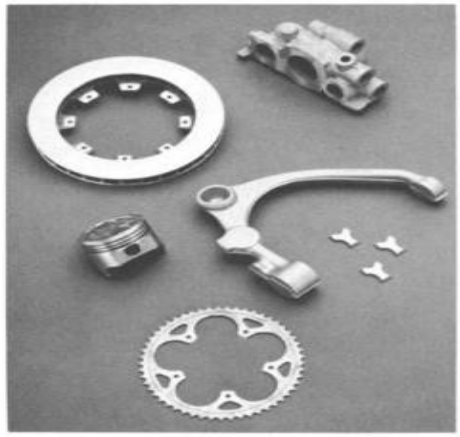

Figure 1.1. Discontinuous silicon carbide/aluminum cast [4].

A ceramic compact composed of aluminosilicate has been used to reinforce a Toyota diesel engine piston, which is currently in production. An all-aluminum piston may sustain wear similar to that of a piston with an iron insert by utilizing a ceramic fiber preform for selective reinforcement, and its thermal conductivity is very slightly lower than that of unreinforced aluminum. A lighter piston with better thermal stability and high-temperature strength is produced by removing the iron component [10].

Based on the kind, form, and technique of their reinforcements, metal matrix composites fall into several different types. Regarding MMCs with aluminum serving as the matrix metal, the following classification is pertinent. In essence, hybrid MMCs are made up of multiple types of reinforcement, such as a combination of fiber and particle, whisker and particle, or hard and soft reinforcements combined. Composites with better mechanical characteristics than carbon have been developed since the discovery of carbon nanotubes [11].

Consequently, by modifying the way materials are processed to meet the requirements in varied working circumstances MMCs offer greater prospects for broader material uses. Finite element modeling techniques can also be utilized to create composite materials that have the desired properties. One can predict the properties of a particular material with a given composition using these techniques. In the same way, materials can be made to have specific qualities by using comparable techniques [8].

The purpose of this study is therefore to review recent works of literature related to the application of aluminum-based metal matrix composites, processing techniques of hybrid MMCs, and wear behavior of these materials and point out some gaps within the literature and then to fabricate and investigate the wear performance of Al6061-$TiBr_2$-Gr composite via stir casting process, and finally to optimize the wear condition of a selected composition.

1.3. STATEMENT OF THE PROBLEM

In Aircraft, being able to evaluate surfaces that touch each other is of vital importance to a failure investigation. For example, the unwanted fretting and wear of hinges, tracks, bearings, and gearboxes in airframes and engines is a constant problem, because it induces failures and jamming [12].

Although aluminum alloy and its composites are essential in many engineering applications, its wear qualities are inadequate [13]. TiB_2-reinforced composite with an aluminum basis shows promise as a brake drum material and could eventually replace traditional gray cast iron [14].

Since wear resistance is a material quality with considerable practical value, it has usually dominated research attention. Although wear is a multidisciplinary phenomenon resulting from concurrent mechanical, physical, and chemical processes, recent developments in advanced material design and development as well as characterization techniques have maintained approaches to understanding and forecasting wear progression [15]. Thus, in addition to hardness, additional contributing factors that affect this complicated phenomenon include the sliding material's mechanical properties, microstructure, processing technique, and thermal properties [14]. Simultaneously, studies have indicated that the incorporation of graphite to Al-based composites has resulted in better wear properties than base alloys; additionally, the graphite content forms a lubricating film on the wear surface and minimizes the wear rate and coefficient of friction, thereby enhancing the matrix's tribological properties [16].

Therefore, this study addresses whether or not the addition of graphite particles to the base material in different volume percentages enhances the wear property of the hybrid metal matrix composite and optimize the wear conditions for the selected best composition of the composite material.

1.4. OBJECTIVES OF THE RESEARCH

1.4.1. GENERAL OBJECTIVE

The general objective of this study is to fabricate, and experimentally investigate the wear resistance of Al-TiB_2-Gr hybrid composite, analyze the effect of graphite addition on the wear performance, and optimize the wear condition of a selected composition.

1.4.2. SPECIFIC OBJECTIVES

The aim of this research is:

- ✓ To fabricate Al-$TiBr_2$ composite with different wt% of Gr using stir casting process.
- ✓ To determine the microhardness of Al-TiB_2 composite for different %wt of graphite.
- ✓ To explore wear resistance of Al-TiB_2 composite for different wt% of Gr using pin-on-disc test.
- ✓ To explore the potential of the addition of Graphite particles to the Al-TiB_2 composite in terms of wear resistance and identify the appropriate composition.
- ✓ To examine the microstructure of the hybrid composite for different compositions
- ✓ To optimize wear condition parameters for a selected composition of the composite.

1.5. SCOPE OF THE RESEARCH

This study starts from a review of different literature related to the title of the research and focuses on experimentally investigating and optimizing the wear properties of the Al-10%TiB_2-Gr hybrid composites and the Microhardness of the composites. The microstructure of the composite's material SEM micrographs were presented for analysis. Experiments were done several times as per the standards with different volume fractions of reinforcements.

In the second phase of the research, among the fabricated samples, the best composition sample was selected for optimization of wear condition using Taguchi analysis in MINITAB v21.2 for better wear performances. The S/N ratio for COF and wear responses were analyzed to show which parameter is significant for the wear condition of the composite.

However, this research was not extended to other mechanical properties of the composite, like impact strength, tensile strength, fatigue, toughness, brittleness, corrosion resistance, and other important properties due to limitations of resources.

1.6. RESEARCH QUESTIONS

- What was the effect of the addition of graphite on the hardness of the hybrid composite material?
- How did the addition of the graphite particle affect the microstructure of the hybrid composite?
- What was the appropriate composition of Al-TiB_2-Gr hybrid composite for a better wear performance?
- What parameters of the pin-on-disk dry sliding wear were optimum for better wear performance of the composite material?

1.7. MOTIVATION OF THE RESEARCH

Many researchers have committed to obtaining new materials for different purposes and different applications. While looking at different literature and reviewing different research works, it is very interesting to work on aluminum-based metal matrix composites. Being able to conduct experiments, analyze the work, and understand the results using all the principles, methods, and knowledge that have been gained throughout the previous education is something that can always be looked at as an achievement and a success.

In addition to acquiring operational knowledge while doing the research, it is also a very big accomplishment to complete the post-graduate program, since this thesis work is a partial fulfillment of for MSc degree.

1.8. SIGNIFICANCE OF THE RESEARCH

The development of hybrid MMCs is driven by the need for innovative wear-resistant materials for high-performance tribological applications, and the matrix alloy characteristics are improved by the inclusion of two or more reinforcements over a single reinforcement.

For instance, for the manufacturing of pistons and cylinder heads, the use of TiB_2, SiC, or graphite-reinforced aluminum alloy composites in the automotive and aerospace industries has been steadily rising. A variety of techniques, including powder metallurgy, the vortex method, infiltration, spray deposition, and squeeze casting, are used to create metal matrix composites. The stir casting process is a well-established method for producing large quantities of aluminum matrix composite that is discontinuously reinforced and has consistent characteristics. Numerous studies have demonstrated that the mechanical, tribological, and machinability qualities of the aluminum alloy were improved by the inclusion of self-lubricating elements like graphite.

Therefore, this research will be a significant piece of work in terms of finding out its influence on the wear resistance of the base Aluminum 6061 and the other reinforcement Titanium diboride particulate, as a hybrid composite.

1.9. THESIS ORGANIZATION

This research paper consists of five chapters. In the first chapter, the introduction and background of the study were presented, the problem statement was formulated, the objectives of the study were defined, and the significance of the study and the scope of the study were also clearly stated. The second chapter reviews literature that is similar to this study and identifies gaps. The third chapter is about materials, methods, and methodologies of fabrication of the composite and investigation of their properties. The fourth chapter presents a detailed discussion and analysis of the experimental results of mechanical and tribological tests and the microstructure of manufactured composite. Finally, the last chapter presents the conclusion, recommendations, and highlights for future works.

CHAPTER TWO

2. LITERATURE REVIEW

2.1. INTRODUCTION

Numerous studies are constantly being carried out to enhance the mechanical characteristics of composite materials without compromising the material's thermal or physical attributes. It has significantly advanced materials used in a variety of applications, and manufacturing technology, material science, and theoretical analysis are all paying more and more attention to them.

The performance and cost of many of the composites utilized today are suitable for highly complex applications like spacecraft, and they represent the cutting edge of materials technology. The selection of materials always has a negative or positive impact on the production process and the overall quality of the product.

Therefore, in this chapter, a lot of related research papers are reviewed that use different techniques, methodologies, and objectives in general. Since the area of interest of this study is ceramic particles reinforced to Aluminum metal matrix, subtopics will focus on metal matrix composites and Reinforcements, particularly related works to Titanium diboride and graphite.

2.2. COMPOSITE MATERIAL

The matrix phase and reinforcing phase of a composite are typically where its unique characteristics develop. Because of this, the properties of composites are frequently in the range between those of reinforcing materials and matrix materials [17]. When compared to traditional materials, composite materials offer better mechanical qualities such as increased fatigue life, corrosion resistance, high specific stiffness and strength, and improved fracture toughness. However, making the most of composites' advantages necessitates careful design and optimization. [18].

Composite materials exhibit superior performance due to their unique characteristics. These qualities allow composite materials to work more effectively [19]. Due to two desirable characteristics, composite materials have been used more frequently recently in mechanical, civil, and aerospace engineering applications: first, they have a high specific stiffness and strength per unit density; second, they are highly flexible, offering designers a great deal of flexibility in terms of how fibers are arranged and stacked [20].

The appropriate selection of materials for power transmission is required by the automotive industry. Enhancing the efficiency of the torsion and bending resistance is the fundamental objective of choosing appropriate materials. **Asiri et al.,** [21] have presented the findings of the carbon fiber composite crankshaft's modal and harmonic analysis. Since carbon composite is known for being stiff, researchers compared it to other materials to see whether it would be the ideal choice for engine shaft development. The models developed in the case underwent many tests, and the composite performed admirably.

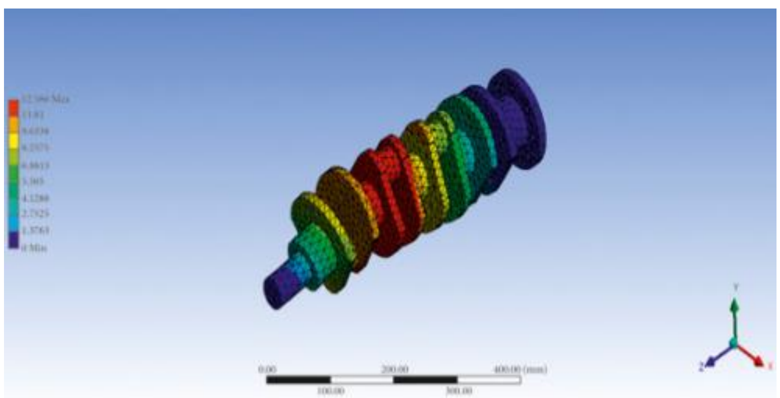

Figure 2. 1. A carbon composite crankshaft modal and harmonic analysis [21].

2.3. CONSTITUTES OF COMPOSITE MATERIAL

2.3.1. MATRIX MATERIAL

Combining two or more materials for producing a material that is better than using the individual components alone occurs as a composite material. In contrast to metallic alloys, every material maintains its distinct chemical, physical, and mechanical properties. A matrix and reinforcement are the two parts. A composite material's low density, excellent strength, and stiffness are its main advantages over traditional materials [20].

The matrix and the reinforcements are the two phases that make up composite materials. In the matrix phase, metals or ceramic polymers are utilized, while in the reinforcing phase, fibers and particles are incorporated. Depending on the application, the discontinuous phase is either softer or harder. Harder reinforcements are utilized in the manufacturing of components that require exceptional wear resistance, whereas softer reinforcements, including graphite and molybdenum, are used to achieve lubricating properties. Composite material properties are determined by the matrix and reinforcements. Even while the reinforcement enhances the matrix's general properties, the matrix itself retains the reinforcement to produce the required form [22].

Reinforcements such as Al_2O_3, SiC, B_4C, TiB_2, Carbon nano-tubes (CNT), and Graphene-nanoplatelets (GNPs) are typically used in the production of magnesium matrix composites. In recent years, researchers have been working to reduce the cost of magnesium matrix composites by utilizing less expensive and environmentally friendly reinforcements. The use of these reinforcements, which can be solid wastes like eggshells, fly ash, red mud, and waste glass, in composite systems is expanding all the time [23].

In addition to the more well-known flaws found in metallic structures, it is crucial to understand that the introduction of composite media has led to the emergence of some new material faults in composite structures. Therefore, broken fibers, delaminated areas, fissures in the matrix material, holes, foreign inclusions, and microscopic voids are examples of material and structural issues that can occur in composite materials. There have always been flaws, and in many situations, they have had a significant impact on a system's structural reaction [19].

2.3.2. REINFORCEMENT MATERIAL

One matrix and two or more reinforcing components make up hybrid materials. They are made using a range of techniques, including powder metallurgy, stir casting, two-step stir casting, and squeeze casting, to achieve the required mechanical properties and tribological behavior including high specific strength, stiffness, density, and microhardness; low coefficient of thermal expansion; high thermal resistance; and excellent damping capacity [24].

Developing hybrid composites with multiple kinds of reinforcement is one of the most efficient ways to improve the characteristics of aluminum alloys. In comparison to monolithic, alloy, and composite materials, hybrid composites have several advantages such as a high strength-to-weight ratio, superior stiffness and strength, resistance to corrosion and wear, low thermal conductivity and thermal expansion, low weight, enhanced impact and flexural properties, and a lower total cost of composites [25].

Compared to conventional structural materials, the strengths and stiffness of the fibers utilized in modern composites are significantly higher. The processing that prevents internal or external texture flaws, which typically compromise glass, is responsible for the high strengths of glass fibers, and the nearly perfect alignment of molecular chains with the fiber axis is what gives polymeric aramid fiber its strength and stiffness [19].

It is common to add more than a single reinforcement material into the metal matrix to enhance the mechanical properties of the material by taking advantage of the excellent qualities of each constituent material.

2.4. CLASSIFICATION OF COMPOSITE MATERIALS

Based on the type of matrix materials used, composite materials can be classified into three groups as shown in Figure 2.2.

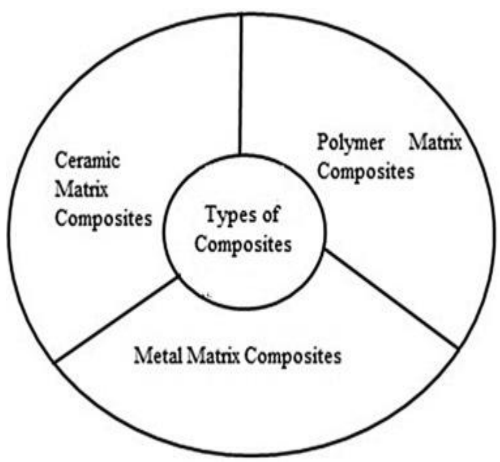

Figure 2. 2. Composite materials classification. [22]

2.4.1. CERAMIC MATRIX COMPOSITE

Ceramic matrices are frequently used for high-temperature applications, such as pistons, blades, and rotors in gas turbine parts. They perform well in corrosive settings and can withstand high temperatures. Since monolithic ceramics are brittle despite having great stiffness and strength, the main objective in the development of ceramic matrix composites is to increase the toughness

[22]. In CMC, ceramic materials are used for both reinforcement and the matrix. While the reinforcement provides distinctive features that make things unique, the matrix material maintains operations applications requiring strong thermal and mechanical properties, ceramic matrix composites emerged as a result of a need in application areas such as aircraft, chemical plants, space building, nuclear power plants, and transportation services.[23].

Ceramic Matrix Composites are solid materials that often exhibit extremely strong bonding, usually ionic but occasionally covalent bonds. They are usually composed of a mixture of ceramic fibers, whiskers, and particles with a matrix of another ceramic. It is possible to reinforce the ceramic matrix with ceramics, metals, glasses, and polymers. The ceramic-based matrix materials exhibit remarkable stability at elevated temperatures, high melting points, improved compressive strength, and corrosion resistance [22].

In the area of machining composites, a great deal of study has been done and recounted across several evaluations. Owing to their distinct shape, CMCs have been deemed difficult for machine operations. Due to the recent rise in demand for long fiber-reinforced CMC, high-temperature structural industries like nuclear power, autos, and aviation are using these materials. The engineered connections between the fibers and matrix in ceramic composites reinforced with long fibers have been developed to provide a controlled bridging approach for cracks. This enhances the fracture toughness of the composites, making them suitable for use in a variety of structural applications, such as nuclear reactors and aero engines. Aluminum oxides, boron carbide, and silicon carbide are amongst the materials with relatively highest modulus of elasticity [27].

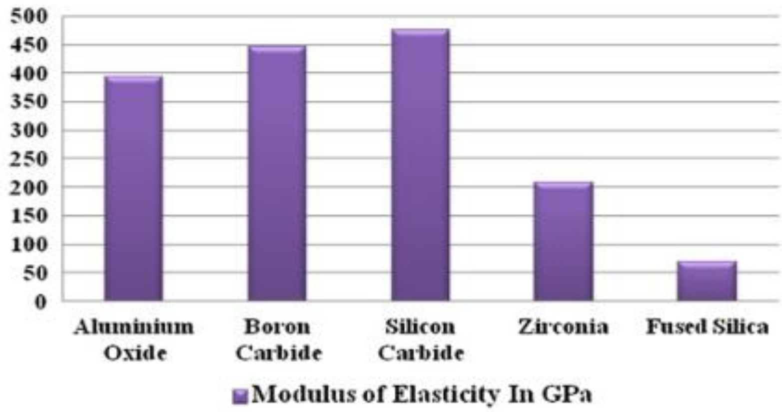

Figure 2. 3. Modulus of elasticity of some common ceramic materials [22].

2.4.2. METAL MATRIX COMPOSITE

Metal matrix composites (MMCs) are often made of low-density metals, like magnesium or aluminum, reinforced with ceramic fibers or particles, including silicon carbide, titanium diboride, or graphite [28].

Because of their excellent heat conductivity, copper and aluminum were frequently utilized as matrices in metal matrix composites. They were strengthened with diamond, SiC, and carbon. The aerospace industry is becoming more and more interested in employing metal matrix composites. These studies have made use of aluminum metal matrix composites because of their enormous potential to produce lightweight, robust components for aircraft. These materials are usually used because they are lightweight and can tolerate the pressures that are produced during operation [29].

Various types of metal matrix composites exist, including refractory, nickel, and aluminum. These metal matrix composites contain fillers made of silicon carbide, titanium carbide, aluminum oxide, and other materials. Metal matrix composites find application in the automotive and locomotive, aerospace and defense, electrical and electronics, industrial, and other end-user industries [30].

2.4.3. POLYMERIC MATRIX COMPOSITE

Since the basic unit of a polymer is composed of carbon, hydrogen, oxygen, and/or silicon, the most basic understanding of a polymer is something comprised of numerous units. Polymers, like shellac and tar, have been a part of human history since the beginning of civilization. They are heated and compressed to create useful products like bearings, bushes, gears, and modern engineering uses. Almost every industry uses polymer materials; both natural and synthetic polymers can be manufactured with a broad range of properties, including stiffness, strength, heat resistance, crystallinity, density, and even cost [31].

Because ceramic fibers are stronger than matrix material, they are typically used in PMCs to reinforce the matrix. The matrix, reinforcement, process parameters, microstructure, composition, and interphase all influence the properties of PMCs. PMCs are widely recognized for their affordable cost and simple manufacturing process [22].

As shown in Figure 2.4., Polymers are classified into two classes according to ASTM D883 80c, which describes their chemical and technical characteristics.

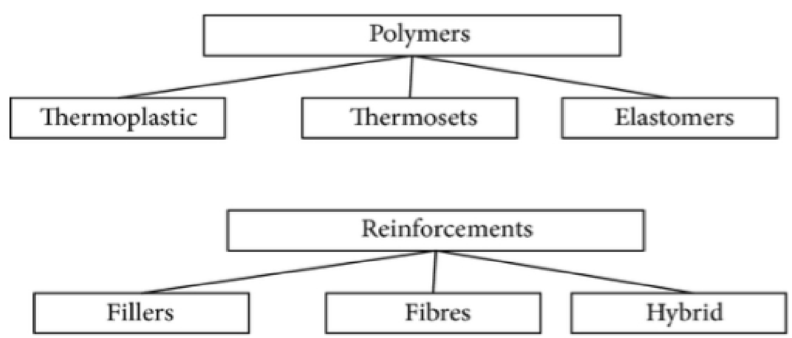

Figure 2. 4. Reinforcements of Polymers Classification. [31]

In polymer matrix composites, a thermoplastic or thermosetting plastic matrix contains one or more reinforcements, such as carbon, glass, steel, or natural fibers. Because polymers are easily manufactured, they yield high-quality components. For polymers, lightweight is a crucial characteristic. The qualities of polymer composite composites, or PCCs, are diverse. Among them are high strength, exceptional impact, compression, and fatigue capabilities; economical production and tooling methods; exceptional resistance to chemicals and corrosion; inexpensive chemical inertness; and good mechanical qualities. PMCs are typically used in sporting equipment, aircraft, and rocketry [22].

2.5. ALUMINUM METAL MATRIX COMPOSITES

Aluminum composites are utilized extensively in the automotive industry Because they are lightweight and resistant to corrosion,[9]. Because of its low weight, density, coefficient of thermal expansion, high strength, and wear resistance, aluminum alloys have seen a sharp growth in use in recent years. When reinforcements are added to the metallic matrix, the properties of stiffness, specific strength, creep, and fatigue are improved in comparison to the traditional materials [28].

Although aluminum alloy and its composites are essential for many engineering applications, their wear characteristics are not excellent. In the alloy matrix, hard reinforcements are uniformly dispersed to enhance the tribological characteristics. Dispersed particles, such as oxides, carbides, and borides which are thermally stable and insoluble at very high temperatures, are usually mixed in the aluminum matrix [13].

To strengthen aluminum and its alloys, ceramic particles are added to make a better-performing composite material. Titanium-based composites are widely used, particularly as building materials for constructions subjected to high temperatures. Titanium alloys are often used in aircraft components due to their outstanding rigidity at elevated temperatures and robust corrosion resistance. But the material costs substantially [22].

2.6. RESEARCH WORKS ON MMCs

A. Thirumoorthy, et.al [30] reviewed the most recent advancements in aluminum matrix research with particulate reinforcement composites. The literature review shown that the mechanical and tribological properties of aluminum-based composites were enhanced by the addition of carbide and oxide-based particle reinforcement. Some researchers have even looked at whether adding fly ash and graphite to aluminum alloys improves their characteristics and their results showed that mechanical properties were improved.

In another study, Titanium diboride (TiB_2) particles were reinforced in an Aluminum (Al) metal matrix via an in-situ salt metal reaction technique. The addition of 8% TiB_2 was shown to improve the mechanical properties of TiB_2-reinforced Al 6061 alloys, mainly tensile strength and hardness, which were found to increase to 172 and 54 N/mm^2, respectively. By using the pin-on-disc method, the samples with the highest weight percentage of reinforcement also exhibit excellent wear resistance. this indicated that high-performance materials utilized in automotive disc brakes have to contend with TiB_2-Aluminum composites [9].

Ravi Kumar V, et.al [32] examined the fabricated composites containing 4% Ni and 2, 4, 6, & 8% SiC as reinforcements in pure Al as a base matrix was successfully achieved with a load of 160kN and sintering temperature was optimized to 530±5 °C. As the amount of SiC in the composites increased the hardness of the materials also increased; the highest increase, of 87%, was seen in the 8% SiC composite. As the amount of SiC increased, the composites' wear resistance considerably improved. A 90% increase in maximum wear resistance was found for the 8% SiC composite. The mechanical and tribological properties of pure Al were therefore effectively enhanced by the addition of SiC to the matrix.

Jaswinder Singh, et.al [33] reviewed the hybrid aluminum matrix composites' characterization for cutting-edge uses. The review noted that the microstructures of the hybrid aluminum matrix composites were stable and had a uniform distribution of reinforcing particles. Fly ash, rice husk ash, mica, and other partial reinforcements increase the density of the composites as the amount of ceramic reinforcement increases. Additionally, it has been noted in the literature that to give the composite the desired qualities, complimentary reinforcements such as SiC or alumina can be added to synthetic reinforcements. The study also shows that in many cutting-edge applications, the composites may be used in place of traditional materials.

2.7. WEAR PROPERTIES OF MMCS

Veeresh Kumar et al. [34] developed Al 7075/SiC composite material by liquid metallurgy route and studied the wear behavior. They laid out that when particle size is inversely proportional to the wear rate, the sliding speed and volume fraction of reinforcement were in proportion to the rate of wear. In their investigation, they found that 6% SiC reinforced composite presented better tribological and mechanical properties in comparison with the base alloy.

This is because the MMC's wear resistance has increased as a result of the presence of SiC and TiC. The sample containing 100% Al 7075, 0% SiC, and 0% TiC attained the largest coefficient of friction value and, in turn, had the lowest microhardness. The phenomenon illustrates how the alloy's wear-resistant qualities are increased when SiC and TiC are incorporated along the aluminum matrix [35].

C. Velmurugan et al. [36] added graphite particles in weight percentages of 1%, 3%, and 5% of silicon carbide particles in weight percentages of 8% to Al 6061 metallic matrix using a stir casting technique. Following the study, there was significant wear at all aging periods for the metal matrix composites containing low-weight fractions of graphite particles. Over 8 hours, base metal exhibited more wear, while metal matrix composites containing 5 weight percent graphite and 8 weight percent SiC displayed reduced wear. During the first wear phase, the reinforced particles serve as load-bearing components and prevent plastic deformation and matrix material adherence. The worn particles become displaced from their places in the matrix and combine with the wear debris in the final phases of the wear regime. With an increase in the weight percentage of reinforcing particles, there has been less wear.

2.8. FABRICATION TECHNIQUES OF MMCS

There are two types of MMC processing methods. The process of producing the composite from its constituent raw materials is commonly referred to as primary processing. It requires obtaining the right bonding of the elements and adding the reinforcement to the matrix in the right amount and location. All the extra procedures required to transform the primary composite into a completed hardware component are referred to as secondary processing. Many matrix and reinforcing materials are not naturally compatible, and processing such elements into a composite requires customizing the interface's properties. In certain composites, there is insufficient coupling between the metal and the reinforcing ingredient, which needs to be improved. Preventing excessive chemical activity at the interface, which could negatively impact the material's characteristics, is a challenge when working with MMCs made of reactive elements. These issues are typically fixed by changing the matrix alloy's composition or by applying the reinforcement a surface treatment or coating [4].

The utilization of continuous fibers as reinforcement has been the main focus of Gr/Al MMC development efforts. Nonetheless, a number of solidification processing methods have been researched for use in producing Gr/Al cast particles for applications requiring an affordable antifriction material. Short fibers, particles, or compacted staple fiber preforms are used as reinforcements in the production of discontinuous Al203/AI MMCs. A castable discontinuous MMC has been created by adding chopped A1203 fibers to an agitated, partially solid aluminum alloy slurry [37][38].

The properties of matrices and reinforcements, as well as the forms, dimensions, and technical specifications of goods and end users, all influence the fabrication process of composite parts. Various techniques for manufacturing and forming are categorized as follows: [28]

- Solid-state methods
  - ✓ Powder metallurgy
  - ✓ Diffusion bonding
- Liquid state methods
  - ✓ Stir casting
  - ✓ Squeeze casting
- In-situ fabrication technique
- Vapor Deposition

2.9. APPLICATIONS OF ALUMINUM METAL MATRIX COMPOSITES

When it comes to their maximum working temperature, matrix composite materials—which are composed of combining two or more components, one of which is a metal—display an essential benefit over their counterparts in organic matrix composites.

Rawal et al. [39] reported that A comparable boron/epoxy composite is only capable of withstanding temperatures of roughly 190°C, while the boron/aluminum composite provides effective mechanical characteristics up to 510°C. Moreover, because of the substantial contribution from the metallic matrix, graphite/aluminum, graphite/copper, and graphite/magnesium composites have better thermal conductivity. By combining the ductility of the matrix with the strength of the reinforcement, a metal matrix composite preserves the advantageous characteristics of both the reinforcement and the matrix [40].

The reinforcing constituent may be a particle, platelet, short fiber, or continuous fiber and may range from sub-micrometer to millimeter in size. There is a difference between metal matrix composites and multiphase metallic alloys as the concept of MMCs introduces additional degrees of Aluminum Alloys and Composites freedom into designing the microstructure. Materials with desirable properties not obtainable by conventional alloying and heat treatment can be created by compositing. This can be achieved by varying the reinforcement type (metallic, ceramic, or polymeric), content (volume fraction), size, shape, distribution, and orientation [41].

Because of its outstanding properties, the metal matrix composite has found extensive application in the aircraft industry [42]. When silicon carbide (SiC) nanoparticles are placed in metals, they show increased hardness, wear resistance, and corrosion resistance. Therefore, aluminum, which is used to construct a range of machine elements such as ventral fins and fuel access covers in aircraft, as well as drive shafts, brake rotors, and brake drums in automobiles, can be merged with nano-SiC particles to reduce wear [43].

Similar to this, nano-titanium carbide has a number of benefits, particularly good wear characteristics, a high specific strength, and corrosion resistance [44]. In addition to these qualities, titanium carbide offers a great strength-to-weight ratio, which is especially important in the chemical, aerospace, and construction fields. According to studies, MMC with SiC/TiC reinforcement improve aluminum's mechanical properties [45].

The preferred material for the fuselage, wings, and supporting components of commercial, military, and cargo aircraft is aluminum alloys and/or composites. Around eighty percent of the weight of a typical modern commercial aircraft is comprised of up of aluminum in the airframe. The International Maritime Organization's high-speed code for vessel design, safety, and fire risk control is satisfied by materials based on aluminum. Aluminum handles the torsional, flexural, compression, and impact loads of high-speed water movement better than steel [8].

2.10. SUMMARY

In summary, Composites are a recent class of structural materials that are gradually taking over the role of traditional materials in a variety of engineering applications because of their decreased density and concurrent improvements in mechanical and tribological performance. Lighter materials must be used specifically for combustion engine applications since they maximize fuel economy and reduce pollution-related issues. Because they can attain a greater strength-to-weight ratio by adjusting the composition and distribution of the reinforcing matrix, metal-based composite materials are shown to be a promising solution to such issues [35].

This chapter attempted to highlight the fundamental aspects of these composite materials and their performance against the conventional metallic class of materials along with the recent development in advanced composite materials. The reviewed literature in this chapter is summarized in Table 2.1.

Table 2. 1. Literature Review Summary.

Author [Reference]	Title	Findings
A. Thirumoorthy, et.al [30]	Review of the Latest research development in Aluminum Matrix with Particulate Reinforcement Composites.	The review of the literature demonstrated evidence that adding carbide- and oxide-based particle reinforcement to aluminum-based composites increased their mechanical and tribological properties.
Himanshu, et al [46]	Mechanical and Tribological Behaviors of Stir Cast Aluminum Matrix Composites.	The microhardness and macro hardness of the composite increased with the amount of Al-N in the alloy matrix, according to the researcher's findings.
Karbalaei et al. [47]	Fabrication and study on mechanical properties and fracture behavior of nanometric Al_2O_3 particle reinforced A356 composites focusing on the parameters of vortex method	examined the mechanical characteristics of an aluminum alloy A356 reinforced with 1.5% nano Al_2O_3, which was produced by stir casting. The composite melt was stirred for 4–16 minutes at 450 rpm and 850^0C casting temperature. The mechanical characteristics of composites were considerably enhanced by the incorporation of nanoparticles. This

		resulted from the aluminum matrix being strengthened by nanoparticle reinforcement and grain refining. As the stirring time was increased, the porosity of the composites increased and the mechanical properties decreased.
Kumar et al. [48]	Synthesis of in situ Al-TiB_2 composites using stir cast route, Composite Structures	Developed an Al-7Si alloy composite reinforced with in situ TiB_2, and examined the wear and mechanical properties of the material. The researchers noted that as the weight percentage of TiB_2 increased, so did the values of hardness, ultimate tensile strength, yield strength, and young's modulus.
Jaswinder Singh, et.al [33]	Review of the Characterization of hybrid aluminum matrix composites for advanced applications	According to the investigation, When fly ash, rice husk ash, mica, and other partial reinforcements are introduced to HAMCs, the density of the composites falls as the amount of ceramic reinforcement increases. Furthermore, it has been shown in the literature that complementary reinforcements, like SiC or alumina, can be added to synthetic reinforcements to obtain the desired properties for the composite.
Stephenson et.al [49]	Development and Applications of Ceramics and New Metal Alloys.	Their findings showed that the graphite particles could be coated with nickel to promote surface wetting during casting.
Radhika et al. [50]	Dry sliding wear behavior of aluminum/alumina/ graphite hybrid metal matrix composites.	The results of their investigation demonstrated that the addition of alumina and graphite particles to composite materials significantly improved their mechanical and wear characteristics when compared to aluminum alloy. The hardness and tensile strength of composites increased as the proportion of reinforcing weight increased. The samples' rate of wear decreased as sliding speed and the weight percentage of alumina particles increased. However, the wear rate increased as well

		when the load increased from 20 to 40 N. With an increase in load and a decrease in velocity, the coefficient of friction increased.
C. Velmurugan et al. [36]	Investigation of friction and wear behavior of hybrid aluminum composites	For the investigation, by using a stir casting technique, graphite particles and silicon carbide particles were added to the Al 6061 metallic matrix in weight percentages of 1%, 3%, 5% and 8%, respectively. The metal matrix composites with low-weight fractions of graphite particles showed considerable wear at all aging times. Base metal showed increased wear over the course of eight hours, but metal matrix composites with five weight percent graphite and eight weight percent SiC showed less wear. There has been reduced wear as the weight percentage of reinforcing particles has increased.

2.11. GAPS IDENTIFIED

The following gaps in the literature and recent research that need to be addressed by further studies are highlighted in this study:

- ✓ According to this study's literature review, only a few studies have been found that investigate the specific tribological pairing of Al 6061 and Gr or TiB_2 and Gr. To completely comprehend that, more research is needed.
- ✓ To acquire an in-depth understanding of this hybrid metal matrix composite, additional experimental testing under different conditions and mix designs is required.
- ✓ There has been minimal effort put into discussing the type of wear and its relationship with the possible plastic deformation of the surface, and the correlation between wear and hardness properties.
- ✓ Studies on the manufacturing of composite materials seem to focus on final products and fabrication methods. But, the effect of porosities and defects during the experimentation should also be given more thought and optimum conditions should be studied more.

CHAPTER THREE

3. RESEARCH MATERIALS AND METHODS

3.1. INTRODUCTION

In this chapter, the necessary inputs to the experimentation process are justified and discussed. From the location of the experimental procedures to the collection of the results and analysis of the data, everything is covered as follows.

The experiments and all of the tests were conducted in the AASTU mechanical laboratory, AAiT mechanical laboratory, ASTU laboratories, and Manufacturing Technology & Engineering Industry Research and Development Center.

Furthermore, the assistance provided by employees of the above institutes, facilities, and research centers has been invaluable in guiding this research work. Their expertise and mentorship have helped to navigate through the complicated process of conducting experiments, and collecting data effectively, enabling to refine the research methodologies and produce good-quality academic work.

The research has two phases. The first phase is the fabrication of the composite and conducting of different tests. The second phase is a selection of one composition from the samples and conducting process parameter optimization of a wear condition.

3.1.1. ASSUMPTIONS

- Equal particle size was considered.
- The interface effect was ignored for metal matrix composite.
- Atomic distribution and orientation of the powders were ignored.

3.2. MATERIALS

In this investigation, an aluminum-based hybrid metal matrix composite containing various combinations of Titanium Diboride and varying weight percentages of Graphite particulate reinforcements of 1 micron and 80 mesh size, respectively, were manufactured by stir casting.

3.2.1. MATRIX MATERIAL

Generally, the following characteristics of aluminum have led to its significance in industrial and commercial applications [8], the majority of which are transferred to its alloys and/or composites.:

- Aluminum is light; with a density of only one-third of that of steel.
- Aluminum is resistant to weather, common atmospheric gases, and various ranges of corrosive liquids.
- Aluminum is safe and can be used in contact with a wide range of foodstuffs.
- It can usually be employed in several decorative applications because of its high reflectivity.
- The strength of aluminum alloys can equal (and sometimes exceed) the strength of the usual construction steel.

In the manufacturing of components in automotive, aerospace, and thermal management industries, particle-reinforced aluminum metal matrix composites made by stir casting, melt infiltration, spraying, and in-situ processing techniques at the industrial level have found success with reinforcements of SiC, Al_2O_3, TiC, TiB_2, and B_4C in. Particle-reinforced Al-MMCs have been employed in the construction of fan exit guide vanes (FEGV) in gas turbine engines. They are also utilized in military aircraft as ventral fins and fuel access cover doors, as well as spinning blade sleeves in helicopters [51].

In a study that investigated the corrosion behavior of Al 7075, Al 2024, and Al 6061, the results showed the following: [52]

- The weight loss data for 32 weeks were consistent with their bimodal model, and the corrosion rates of Al alloys reduced over time.

- A temperature rise resulted in a decrease in corrosion potential as well as an increase in anodic and cathodic current density. The expansion of the passivity region with temperature was linked to a decrease in corrosion potential and an increase in breakdown potential.
- All of the alloys had pitting corrosion, with Al 7075 having the worst corrosion. The most corrosion resistance was demonstrated by Al 6061 during every immersion period.

Following steel, aluminum alloys Al6061 are the second most commonly used structural material. Approximately one-third of steel's density (7.83 g/cm^3) occurs in aluminum (2.7 g/cm^3) [53].

Therefore, Al 6061 is the matrix material used in this study as a result of all of these advantages. The weight percentage composition of each alloy element along with the standard range of values for each element is given in Table 3.1.

Table 3. 1. Composition of Al 6061 Matrix material.

Elements	Mg	Si	Fe	Cu	Mn	Cr	Zn	Ti	Al
Standard value	0.8-1.2	0.4-0.8	≤0.7	0.15-0.4	≤0.15	0.04-0.35	≤0.25	≤0.15	-
Weight %	1.068	0.62	0.498	0.256	0.109	0.116	0.115	0.026	97.15

The Aluminum alloy was purchased from MING TAI Aluminum Products in Zhengzhou, Henan, China. The product quality certificate is provided in APPENDIX I.

Figure 3.1. Al6061 matrix material prepared for fabrication of the composite.

3.2.2. REINFORCEMENTS

Titanium Diboride (TiB_2):

Titanium diboride (TiB_2) is renowned for being a fine powder that can vary from dark grey to black and has a hexagonal crystal structure. It is a ceramic material with reasonably high strength and durability, as seen by the high values of its hardness, strength-to-density ratio, wear resistance, and melting point [54].

However, it appears that the current uses of this material are limited to specialized applications in fields like crucibles, impact-resistant armor, cutting tools, and wear-resistant coatings. Utilizing TiB_2 cathodes in the electrochemical reduction of alumina to aluminum metal is a significant emerging application. If TiB_2 electrical discharge machining is accomplished, more uses might emerge quickly. Economic considerations, especially the price of densifying a material with a high melting point and concerns about the substance's unpredictability, may prevent this material from being used more widely [55].

Angadi et al. [56] effectively investigated how TiB_2 particles affected TiB_2/Al MMC processing parameters to satisfy production needs and looked for the best processing conditions for these metal matrix composites, taking a variety of factors into account. Following the identification of the optimal cutting velocity, feed rate, and depth of cut, the end-process variables—surface roughness and material removal rate, or MRR—were evaluated. The results show significant deviations from the use of titanium diboride nanoparticles for reinforcing Metal Matrix Composites (MMCs).

There are several research and experimental investigations done using titanium diboride as their main reinforcement material. The mechanical properties of this reinforcement material are shown in Table 3.2.

Table 3. 2. Mechanical properties of TiB_2 [48].

Properties	TiB_2
Density ($g\ cm^{-3}$)	4.52
Melting point (°C)	3225
Hardness, Vickers (GPa)	25–35
Modulus of elasticity (GPa)	560
Thermal conductivity ($W\ m^{-1}\ K^{-1}$)	60–120
Crystal structure	Hexagonal

Kwon et al. [57] conducted sliding wear tests on bulk Cu–TiB_2 composites that had different TiB_2 contents (2.5, 5, and 10wt%). A planetary ball mill was used to combine elemental powders of Ti, B, and Cu before undertaking self-propagating high-temperature synthesis (SHS). The Cu–10wt% TiB_2 composite exhibited the lowest wear rate of 0.66mm3/N-m and the highest hardness of 0.9GPa.

Gopalakrishnan et al. [58] fabricated an aluminum matrix composite reinforced with 10% weight percent TiB_2 particles. In comparison to base metal and as-cast composites, it was found that the extruded composites showed better mechanical properties.

Using computer-aided cooling curve analysis, Yang et al. [59] also studied the impact of Lanthanum (La) on the microstructure and corrosion behavior of $TiB_{2(p)}$/Al–Cu composites. For their experiments, the composition of the base materials used was 10%$TiB_{2(p)}$/Al–5%Cu.

Therefore, for this study, Al6061 and 10wt% of TiB_2 are used as a base material for a better and optimal mechanical property of the hybrid metal matrix composite to investigate the addition of graphite particles' effects on the composites.

Figure 3. 2. Reinforcement materials and equipment.

Graphite (Gr):

Increased reinforcing often results in a decrease in the coefficient of friction and an increase in wear resistance for metal matrix composites. Numerous researchers have attempted to examine how graphite particle reinforcement affects the mechanical characteristics of the composite and have found that it is essential to the composite's performance. To lighten the composite's weight while maintaining a reasonable level of performance, it would be worthwhile to investigate hybrid composites [60].

According to research on Al6061-Albite and Al6061-Graphite, increasing the quantity of Gr filler led to better elongation, modulus, and strength at lower hardness. Increasing the amount of albite filler further resulted in higher UTS and hardness with lower ductility [61].

One of the reinforcing components in a polymeric hybrid composite was fine graphite particles of 98% extra pure sized 60 mesh size (the average particle size of the graphite powder was 250 µm) [62].

Sharma et al. [63] examined the wear behavior of Al 6061 reinforced with graphite particles using a liquid casting technique. The reinforcements were added to the melt while stirring at 550 rpm for 10 minutes. A dry sliding wear test was performed using a pin-on-disc apparatus with a variable velocity range of 0.4 – 1.2 m/s, a load of 15–45 N, and a constant sliding distance of 1200 m. The results indicated that the addition of graphite particles significantly increased the mechanical and wear properties of composites when compared to the unreinforced alloy.

In order to reduce porosity development in the composite, achieve better uniform reinforcement distribution, and facilitate appropriate densification of the fabricated composite, the weight percentage composition of any reinforcement addition should not exceed 30% [64]. Therefore, the maximum reinforcement for this research study was 15 wt% (12%SiC, 1%Gr and 2%Cr).

3.2.3. WEIGHT (IN MASS) CALCULATION FOR MATRIX AND REINFORCEMENTS

The total mass of matrix and reinforcements required to fabricate the Al6061-TiB_2-Gr composite samples is found from the total specimens required for hardness test, microstructural examination, and wear test processes. The total volume of the molten metal is decided based on the consideration of the specimen size that is needed, the scrap that will be wasted during the turning operation, the overflow of molten metal during pouring, allowances, and other wastes.

It was desired for all samples to be fabricated with a 25 mm diameter and a 20 cm length. The molten metal's total volume, after accounting for all of these factors, was 100 cm^3. Therefore, the following formula may be used to determine the mass of the reinforcements and the matrix for each sample:

Given:

$$V_T = 100 cm^3$$
$$\rho_{Al} = 2.71 g/cm^3$$
$$\rho_{TiB2} = 4.52 g/cm^3$$
$$\rho_{Gr} = 2.26 g/cm^3$$

$$M_{Reinforcement} = V_{Total} \times \rho_{Reinforcement} \times (\text{Weight percentage}/100) \qquad \text{Eq 3.1}$$

Sample 1: Al6061 + 10%TiB_2

$$M_{Al} = V_T \times \rho_{Al} \times wt\% = 100 cm^3 \times 2.71 g/cm^3 \times 0.9$$
$$= \underline{243.9g}$$
$$M_{TiB2} = V_T \times \rho_{TiB2} \times wt\% = 100 cm^3 \times 4.52 g/cm^3 \times 0.1$$
$$= \underline{45.2g}$$

Sample 2: Al6061 + 10%TiB_2 + 2% Gr

$$M_{Al} = V_T \times \rho_{Al} \times wt\% = 100\ cm^3 \times 2.71\ g/cm^3 \times 0.88$$
$$= \underline{\underline{238.5g}}$$
$$M_{TiB2} = V_T \times \rho_{TiB2} \times wt\% = 100\ cm^3 \times 4.52\ g/cm^3 \times 0.1$$
$$= \underline{\underline{45.2g}}$$
$$M_{Gr} = V_T \times \rho_{Gr} \times wt\% = 100\ cm^3 \times 2.26\ g/cm^3 \times 0.02$$
$$= \underline{\underline{4.52g}}$$

Sample 3: Al6061 + 10%TiB_2 + 4% Gr

$$M_{Al} = V_T \times \rho_{Al} \times wt\% = 100\ cm^3 \times 2.71\ g/cm^3 \times 0.86$$
$$= \underline{\underline{233.06g}}$$
$$M_{TiB2} = V_T \times \rho_{TiB2} \times wt\% = 100\ cm^3 \times 4.52\ g/cm^3 \times 0.1$$
$$= \underline{\underline{45.2g}}$$
$$M_{Gr} = V_T \times \rho_{Gr} \times wt\% = 100\ cm^3 \times 2.26\ g/cm^3 \times 0.04$$
$$= \underline{\underline{9.04g}}$$

Sample 4: Al6061 + 10%TiB_2 + 6% Gr

$$M_{Al} = V_T \times \rho_{Al} \times wt\% = 100\ cm^3 \times 2.71\ g/cm^3 \times 0.84$$
$$= \underline{\underline{227.64g}}$$
$$M_{TiB2} = V_T \times \rho_{TiB2} \times wt\% = 100\ cm^3 \times 4.52\ g/cm^3 \times 0.1$$
$$= \underline{\underline{45.2g}}$$
$$M_{Gr} = V_T \times \rho_{Gr} \times wt\% = 100\ cm^3 \times 2.26\ g/cm^3 \times 0.06$$
$$= \underline{\underline{13.56g}}$$

Sample 5: Al6061 + 10%TiB_2 + 8% Gr

$$M_{Al} = V_T \times \rho_{Al} \times wt\% = 100\ cm^3 \times 2.71\ g/cm^3 \times 0.82$$
$$= \underline{\underline{222.22g}}$$
$$M_{TiB2} = V_T \times \rho_{TiB2} \times wt\% = 100\ cm^3 \times 4.52\ g/cm^3 \times 0.1$$
$$= \underline{\underline{45.2g}}$$
$$M_{Gr} = V_T \times \rho_{Gr} \times wt\% = 100\ cm^3 \times 2.26\ g/cm^3 \times 0.08$$
$$= \underline{\underline{18.08g}}$$

Sample 6: Al6061 + 10%TiB_2 + 10% Gr

$$M_{Al} = V_T \times \rho_{Al} \times wt\% = 100\ cm^3 \times 2.71\ g/cm^3 \times 0.8$$
$$= \underline{\underline{216.8g}}$$
$$M_{TiB2} = V_T \times \rho_{TiB2} \times wt\% = 100\ cm^3 \times 4.52\ g/cm^3 \times 0.1$$
$$= \underline{\underline{45.2g}}$$

$$M_{Gr} = V_T \times \rho_{Gr} \times wt\% = 100\ cm^3 \times 2.26\ g/cm^3 \times 0.1$$
$$= \underline{\underline{22.6g}}$$

3.3. METHODS

3.3.2. FABRICATION OF THE COMPOSITE

Stir casting:

Currently, the most basic and economically feasible way of manufacturing metal matrix composites is by stir casting processes. For this process, the reinforcing particle must be mechanically mixed with a molten metal bath before being transferred to a formed mold and allowed to solidify completely. A feeding mechanism for ceramic particles, a resistance-heating furnace for melting the base metal, and an electrical motor-driven mechanical stirrer for combining the pre-heated particles with the matrix liquid make up the experimental setup [1][26].

The double stir casting, or two-step mixing method, is the most current fascinating development. This procedure involves heating the matrix material over its liquidus temperature and then cooling it to a temperature that falls between the solidus and liquidus points, resulting in a semi-solid state. At this point, preheated reinforcement particles were introduced and combined. For ten minutes, the stirrer's speed was kept constant at 450 RPM. After reaching a fully liquid temperature, the slurry is vigorously stirred once again. The molten composite was then prepared for transferring into the mold box. [1][26].

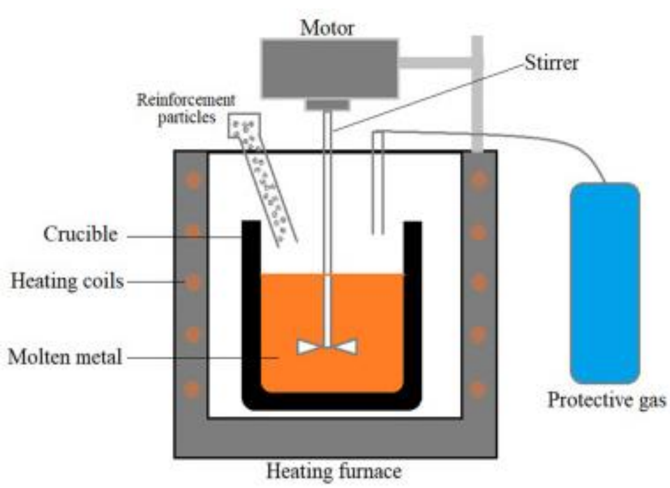

Figure 3.3. Stir casting setup [23].

Table 3.3. illustrates the compositions of the cast hybrid composites. Previous studies on Al-TiB_2 composites have shown a similar trend due to its optimal weight percentage in the matrix material [36] [65] [66] [67].

Table 3.3. The cast Hybrid composites and their compositions [36].

No	Specimen composition
1	Al 6061 + 10% TiB_2 + 0% Gr
2	Al 6061 + 10% TiB_2 + 2% Gr
3	Al 6061 + 10% TiB_2 + 4% Gr
4	Al 6061 + 10% TiB_2 + 6% Gr
5	Al 6061 + 10% TiB_2 + 8% Gr
6	Al 6061 + 10% TiB_2 + 10% Gr

Stirring parameters:

The stirring time and speed, the impeller (size, shape, and position in the melt), the shear rate, the shear period, the cooling rate, and the volume fraction of primary solid are all crucial factors in any stir casting method used for MMCs or MMNCs. The stirrer's ideal diameter (d) and width (b), where D is the crucible diameter, have been reported to be 0.4D and 0.1–0.2D, respectively [68].

The stirring speed determines the formation of a vortex, which is responsible for dispersing particles in liquid metal. According to studies, the ideal speed range is between 300 and 600 rpm [69]. For this process, the stirring speed was 450 rpm.

In general, stirring at rates less than 100 rpm and more than 600 rpm is not suggested. A poor mechanical property is anticipated when a speed exceeds 600 rpm because it typically leads to unfavorable outcomes including excessive turbulence, pollutants, gasses, and oxide absorbance from the atmosphere [68]. More particles with longer durations are embedded and lodged in the metal matrix at optimum speed [70].

Figure 3.4. Molten composite material in the furnace at 629^0c.

Based on a simulation and experiments, **Krishnan et al.** [71] concluded that the optimal arrangement for achieving the optimum microstructural and mechanical properties in Al MMCs is a four-blade flat stirrer. They verified the aforementioned conclusion, according to which the four-blade impeller is suggested due to its higher efficiency. Thus, for this procedure, a four-blade flat stirrer was used.

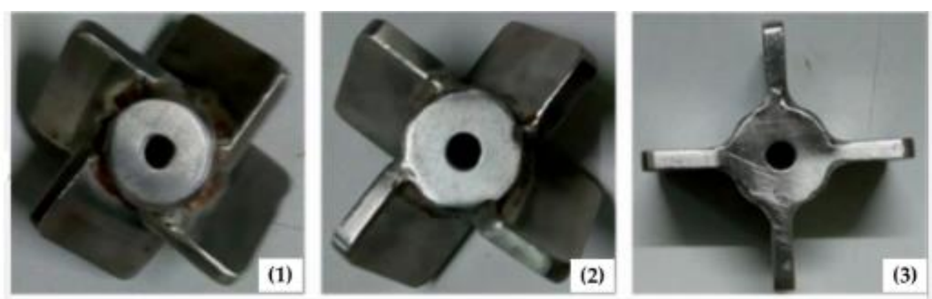

Figure 3.5. Stirrer blades with (1) 45◦, (2) 60◦, and (3) 90◦ [68].

Sand mold:

The sand was dried for several days prior to use for this procedure. The three main procedures for making the mold were selecting an appropriate pattern which is a round bar, filling and ramming the sand, and carefully removing the pattern. Proper preparation of the sand mold, including molding sand selection, compacting, and ensuring adequate venting for gas escape during pouring, is crucial to achieving a defect-free cast. The patterns were prepared from wood and an allowance of 3mm was added to it according to ASTM guidelines for the preparation of composite specimens.

The sand mold, with its unique female die configuration, presents a challenging yet rewarding environment for pouring the molten aluminum composite.

Figure 3.6. Sand mold prepared for casting of composites.

Pouring parameters:

The actual pouring process involved carefully and precisely controlling the pouring temperature to avoid premature solidification. The flow characteristics of the molten composite, influenced by factors such as viscosity, alloy composition, and pouring rate, were properly managed to prevent defects like air entrapment.

Figure 3.7. Molten metal poured in the sand mold and the cooled composite specimen.

The two aluminum pouring temperature parameters that have the greatest impact on the mechanical characteristics and casting-ability of aluminum alloys are the melting and pouring temperatures. As with the melting temperature, the pouring temperature for aluminum must be optimal—that is, not too high, nor too low—to ensure the quality of the casting part. It has been observed that the ideal temperature range for pouring aluminum alloys is between 680°C and 750°C. Additionally, 2.2 to 2.8 cm/s is the optimal pouring speed range for aluminum alloys [72] [73].

Machining of the composites:

Test specimens were prepared by lathe-machining the hybrid composites after they were cast using the stir casting technique. The dimensions of each specimen were 20 mm in diameter and 180 mm in length [38]. The cutting tool reduced the rotating workpiece's diameter to the appropriate dimension by removing material from its outer diameter during the turning operation.

Figure 3.8. Turning operation on the samples.

3.3.1. MORPHOLOGICAL STUDY OF CONSTITUENT MATERIALS

A particle's form, shape, and chemical and physical makeup are all described by its particle morphology. An essential source for details regarding a material's characteristics and its uses in real-world applications is its particle morphology and form analysis.

The microstructure of a composite has a significant impact on its overall performance. However, the microstructure, reinforcing particle size, shape, and distribution within the composite all affect the physical properties of the composites [74]. The micrograph or SEM was able to show:

- Discontinuity
- Interfacial bond
- Wettability
- Porosity
- etc …

Understanding the processing and fabrication of the composite as well as the distribution of the reinforcing particles was the primary goal of the morphology testing.

The reinforcement ceramic powders were prepared for the test using the standard procedure, which resulted in good-quality images of the reinforcements' morphology with a scanning microscope JSM-840A SEM (JEOL Company). JSM-840A is capable of imaging at higher magnifications than optical microscopes, offering the user a range from 5x to 600,000x magnification. It also has the ability to obtain topographical data, useful for physical measurements. JEOL JSM 840A has a scanning electron beam that scan over the sample, allowing for improved bremsstrahlung resolution (radiation given off by free electrons) compared to other SEMs [75].

Figure 3.9. JEOL JSM 840A SEM machine.

The mean grain size of the reinforcement materials was determined by measuring images of the polished and etched surfaces of the materials. The commercially available software, ImageJ, was used. It is a Java-based image processing software that was released by the National Institutes of Health and the Laboratory for Optical and Computational Instrumentations.

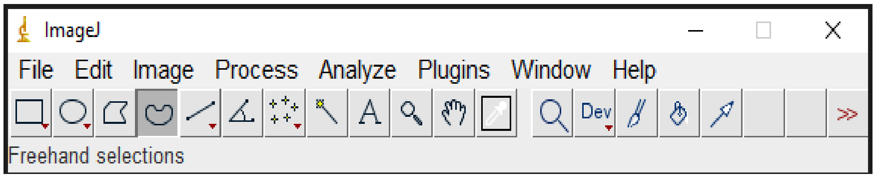

Figure 3.10. Image processing software.

3.3.3. MICROHARDNESS TESTING

The Microhardness tests were conducted according to **ASTM E384-22** standards. A Vickers (DPH) diamond indenter is pushed into the material's surface using an indenter and a small amount of force—a few kilograms—during the microhardness test. When the penetrator is used to apply a load, the material surface becomes permanently deformed or indented due to the indenter's diamond-like shape. The material hardness can be determined using the Knoop and Vickers hardness test procedures, which both require formulas and precise measurements from the indent. Because of their small size, the resulting indentation can only be accurately measured with a specialized microhardness testing microscope. The experiment was carried out at room temperature (30°C), and each sample's hardness was measured at various points to obtain an average value [75] [76].

Figure 3.11. MicroVickers' hardness testing machine.

For this study, the MicroVickers' hardness test machine was used as shown in Figure 3.11. The quotient obtained by dividing the load (kgf) by the square millimeter indentation area is the Vickers hardness value. All of the Al6061-TiB_2-Gr composite specimens have been tested through this experimentation, incorporating 0, 2, 4, 6, 8, and 10 weight percent of reinforcement for the casts. The prepared specimens are shown in APPENDIX IV.

Table 3. 4. Test parameters for Vickers' hardness [77].

Indenter	Angle	Load	Time	Trials
A diamond-like tip with a pyramid shape	$136^{o}C$	2kgf	10 seconds	3

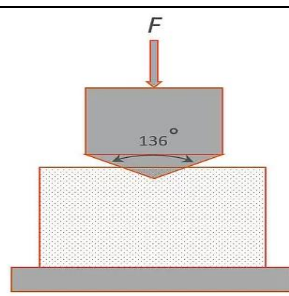

Figure 3.12. Illustration of Vickers' hardness indentation area.

A load of 2kgf was applied progressively for 10 seconds at three distinct places, to obtain average values. After that, the resulting indent mark was viewed optically at a 10x magnification to measure the diagonal lengths and calculate the hardness value. Following that, the VHT machine automatically calculated and displayed the HV number using Eq. 3.1 as stated in ASTM E384-17 [77].

$$\mathrm{HV} = \frac{\text{Constant} \times \text{Force}}{\text{area of indentation}} = \frac{0.102\ x\ 2F\ x\ Sin(\frac{136°}{2})}{D^2} \qquad \text{Eq. 3.1}$$

$$= 0.1891 \times \frac{F}{D^2}$$

Where HV is Vickers hardness value (kgf/mm^2), F is the applied load (Kgf) using the indenter, and D is the average length in millimeters of the diagonals (d_1 & d_2) marked by the indenter.

3.3.4. MICROSTRUCTURAL EXAMINATION

Scanning electron micrographs of stir-cast composites with varying graphite reinforcing concentrations were taken. During the stir casting process, Gr particles are added to the base material, increasing the amount of reinforcement particles.

To achieve an appropriate surface finish, the specimen will first be polished and grinded using several grades of emery sheets before to the microstructural examination. Below is an explanation of the processes:

Grinding is the procedure for smoothing and cleaning the surface that will be examined. A graded sequence of abrasives is used to abrade the specimen's surface for examination, starting with a coarse grit. samples were grinded using the sandpaper of gradually increasing scale 400, 800, and 2000 grits.

Etching is a method for creating contrast on specimen surfaces between microstructural properties. Etching is a regulated process of corrosion that takes place between surfaces with various electrochemical potentials. The samples were grinded, polished, and then etched using an etchant solution (25ml ammonia hydroxide, 20ml hydrogen peroxide, and 25ml distilled water) before to carrying out the suggested microstructural characterization. The samples were merely immersed in the solution for 30 seconds to carry out the etching process.

These processes allow for the achieving of a higher level of surface finish, allowing for a clear view of the hybrid reinforcement particles on the matrix alloy.

Figure 3.13. SEM examination samples.

Therefore, similar procedures were taken in this examination and after the test, the mean size of the grains was measured using **ImageJ software**. The micrograph was drawn by a randomly chosen straight line, which also allowed to count the number of grain boundaries that the line intersects.

3.3.5. PIN-ON-DISC DRY SLIDING WEAR TEST

Tribometers can be utilized for investigations of how material pairings wear and their friction. A predetermined standard force is applied to move a test object—such as a steel ball or pin—over the specimen in a circular motion. The coefficient of friction or the friction force, is constantly recorded throughout the test. Measuring the test specimen's abrasion and wear track allows for the subsequent measurement of wear [78].

Figure 3.14. shows a schematic drawing of a typical pin-on-disk wear test system. A lever-arm device to hold the pin, a driven spindle and chuck to hold the rotating disk, and attachments that allow the pin specimen to be pressed against the rotating disk specimen with a regulated load comprise one sort of typical system. A pin rotating about the disk center is loaded against a stationary disk in a different kind of mechanism. Regardless, the disk's wear track is a circle with

several wear passes on a single track. The system has a mechanism for detecting friction force, like a load cell, which makes it possible to calculate the coefficient of friction.

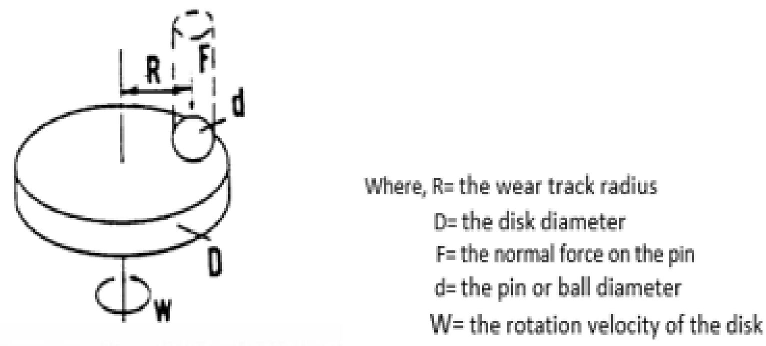

Figure 3. 14. An illustration of a pin-on-disk wear test system [79]

To determine the coefficient of friction and the wear rate of the composites, **Tribometer TR-20 Micro** was used. With the use of this apparatus, the pin-on-disk method of studying material wear behavior can be conducted. It can be programmed to analyze friction in relation to temperature, load, speed, and wear. The apparatus facilitates the mounting of round or square specimens that drive a six-millimeter steel ball. It is equipped with an EN31 carbon steel disk that is 100 mm in diameter and has a hardness of 65 HRC [80].

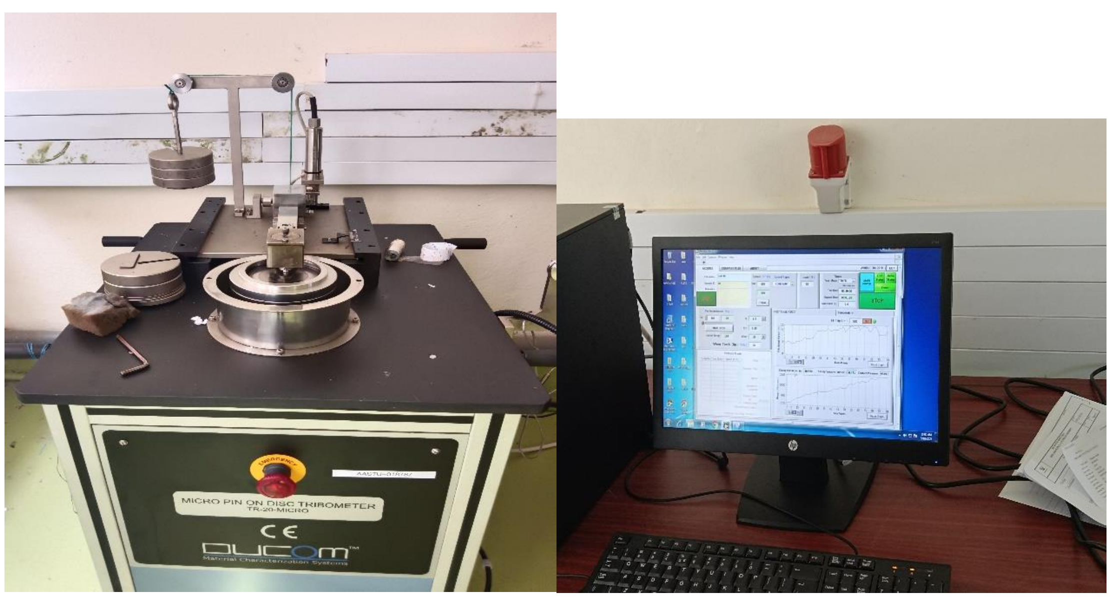

Figure 3.15. A Pin-on-disc apparatus with its data acquisition system.

The samples were weighed accurately with a balance of the fourth decimal. Wear tests using pin-on-disc dry sliding were performed on the composite specimen. During each experiment, the wear loss in microns was measured, and the volumetric wear loss was computed using the weight loss resulting from the wear.

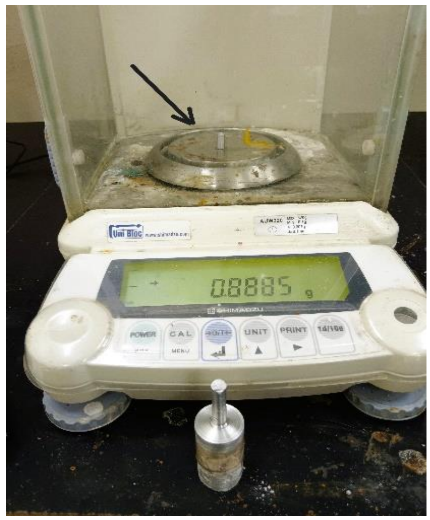

Figure 3.16. A 4-digit UniBloc Analytical balance.

Dimension of specimens:

As per the standards for Tribometer TR-20 tests, the specimens were 12 mm in length and 6 mm in diameter. All samples were carefully cleaned using 50 percent alcohol and petroleum ether before the test began.

Figure 3.17. Samples prepared for experimental tests.

Procedures:

According to ASME G99-95a, the standard guidelines were adhered to. Immediately before testing, specimens were cleaned and dried thoroughly, removing dirt and foreign matter. Cleaning agents and solvents were applied.

Measurements were taken of the specimens to the closest 2.5 µm or 0.0001 g of weight. Then, disks and pin specimens were securely inserted in the holding devices, ensuring they are perpendicular to the disk axis. The system lever or dale was then loaded in order to exert the force that pressed the pin against the disk. The motor was turned on and its speed was varied while the pin specimen was kept away from the disk. The revolution counter was then set to the desired number of revolutions. Lastly, after the predetermined number of revolutions, the test with specimens in contact under stress was completed.

Finally, Specimens were taken out and cleaned from the loose wear debris once the test completed, and features like misplaced metal, spotting, microcracking, or discoloration were identified. Then, the last and most important task was remeasuring specimen dimensions or weighing them and recording them. For the rest of the other specimens and statistically accurate results, a similar procedure was followed.

Parameters of the process:

Vedrtnam and Kumar et al., [81] examined the wear characteristics of aluminum reinforced with copper and silicon carbide. The research revealed that the weight percentage of the reinforcements had the greatest impact on the composite's wear rate. In terms of influence, load and sliding speed came in second and third place, respectively, while sliding distance had the least impact.

Azad and Priyan et al., [82] examined the impact of boron carbide on AA6061 alloy using a stir casting technique, as well as the wear resistance and hardness of composite materials. The authors found that increasing weight percentage of reinforcement to AA6061 alloy increased the hardness and wear resistance of composites. When the samples were evaluated at higher loads, wear tracks of higher weight percentage composites revealed deep grooves with delamination and fine grooves on the surface parallel to the sliding direction.

At higher loads, the wear rate of Al-alloys increases significantly. Al-alloy does not participate directly in the wear process at low loads since the particles serve as load-bearing constituents [83]. Because of a lower real contact area, metallographic measurements at low loads suggested that the composite and counter-face had less chemical interaction [84]. The size of the worn debris is in the order of millimeters at higher weights and a few hundred micrometers at lower loads [85].

Krishnamurthy et al., [86] also studied that the specific wear rate of the aluminum alloy has shown an increase significantly at increasing loads on the Al6063–TiB_2 composites but decreased upon the addition of TiB_2 particles.

Therefore, in this study, optimum parameters from works of literature are adopted. In Table 3.5., the summary of the process parameters is presented.

Table 3.5. Input process parameters for the wear test.

Parameters	**Value**	**Reference**
Applied Load	30N	Krishnamurthy et al. [86]
Sliding Velocity	0.47m/s	
Wear track diameter	30mm	
Disk speed, RPM	300rpm	
Temperature and Humidity	Room temperature	

3.3.6. DESIGN OF EXPERIMENT (DOE)

For the second phase of the study, which was an optimization of the wear conditions of the composite specimen, the Taguchi method was used. The specimen that was selected for this experiment was Sample 5 (Al 82% + TiB2 10% + Gr 8%).

In this study, A DOE model has been created using MINITAB v21.2, and its statistical analysis using Taguchi analysis was carried out to examine the impact of process factors. One of the most widely used and efficient optimization strategies available today is Taguchi's method, which produces a high-quality system using orthogonal array (OA) trials that generate several reduced experiments with the ideal setup for process control parameters. It converts the experimental results into a signal-to-noise (S/N) ratio. Three types of S/N ratios are typically used. nominal-the-best, higher-the-better, and smaller-the-better [87] [88].

The purpose of the design of experiments was to investigate the wear behavior of the composites for different test conditions. The experiments were run in an ambient setting with a variable sliding speed, time, and load (contact pressure). The pin-on-disc equipment was used to conduct the test. On the combination of Al6061 + 10%TiB2 + 8%Gr, experiments were conducted for three distinct factors: load (N), disk speed (RPM), and time (min). These input parameters are thought to be the main design components. Table 3 illustrates the three levels into which each factor was subdivided. In this investigation, a predesigned orthogonal array named L9 (3^3), created by Taguchi, was utilized after taking these experimental conditions into account. An orthogonal array is used in this study which is listed in Table where test conditions and test parameters are represented by rows and columns, respectively. The two output responses, wear and coefficient of friction (COF), are measured using a pin-on-disc instrument. Both output responses meet the same criterion, i.e., a lower value is preferred. Additionally, by using the traditional Taguchi approach, the best parameter settings for each performance characteristics were determined [89].

The three factors (Load, Disk speed, and Sliding Time) were added to MINITAB v21. Since these parameters had three levels, a total of nine runs were made in order to produce a DOE model.

Table 3. 6. Number of experimental runs for 3 factors and 3 levels DOE.

No of Runs	Load (N)	Disk speed (RPM)	Time (min)
1	20	200	5
2	20	300	10
3	20	400	15
4	30	200	10
5	30	300	15
6	30	400	5
7	40	200	15
8	40	300	5
9	40	400	10

3.4. SUMMARY

In Summary, the study used a stir stir-casting technique to fabricate test specimens. Following specimen preparation in accordance with the standards, Wear test by a pin-on-disc technique, Morphological analysis, Microhardness test, and Microstructural examination were conducted.

The second phase of the study was choosing one composition of the composites and conducting optimization of wear parameter conditions. Figure 3.18. shows the general workflow of this study.

Phase one:

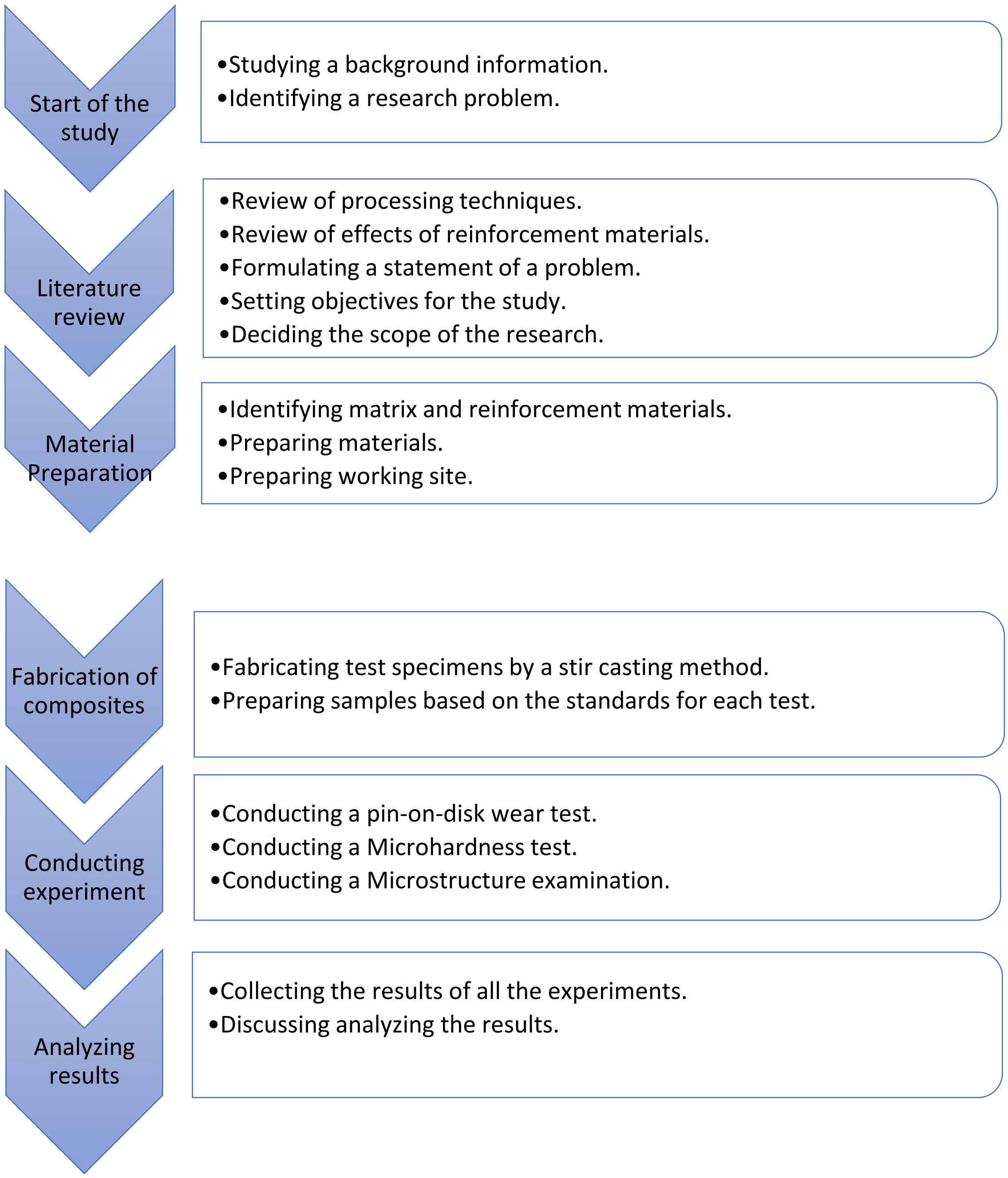
Start of the study
•Studying a background information.
•Identifying a research problem.
Literature review
•Review of processing techniques.
•Review of effects of reinforcement materials.
•Formulating a statement of a problem.
•Setting objectives for the study.
•Deciding the scope of the research.
Material Preparation
•Identifying matrix and reinforcement materials.
•Preparing materials.
•Preparing working site.
Fabrication of composites
•Fabricating test specimens by a stir casting method.
•Preparing samples based on the standards for each test.
Conducting experiment
•Conducting a pin-on-disk wear test.
•Conducting a Microhardness test.
•Conducting a Microstructure examination.
Analyzing results
•Collecting the results of all the experiments.
•Discussing analyzing the results.

Phase two:

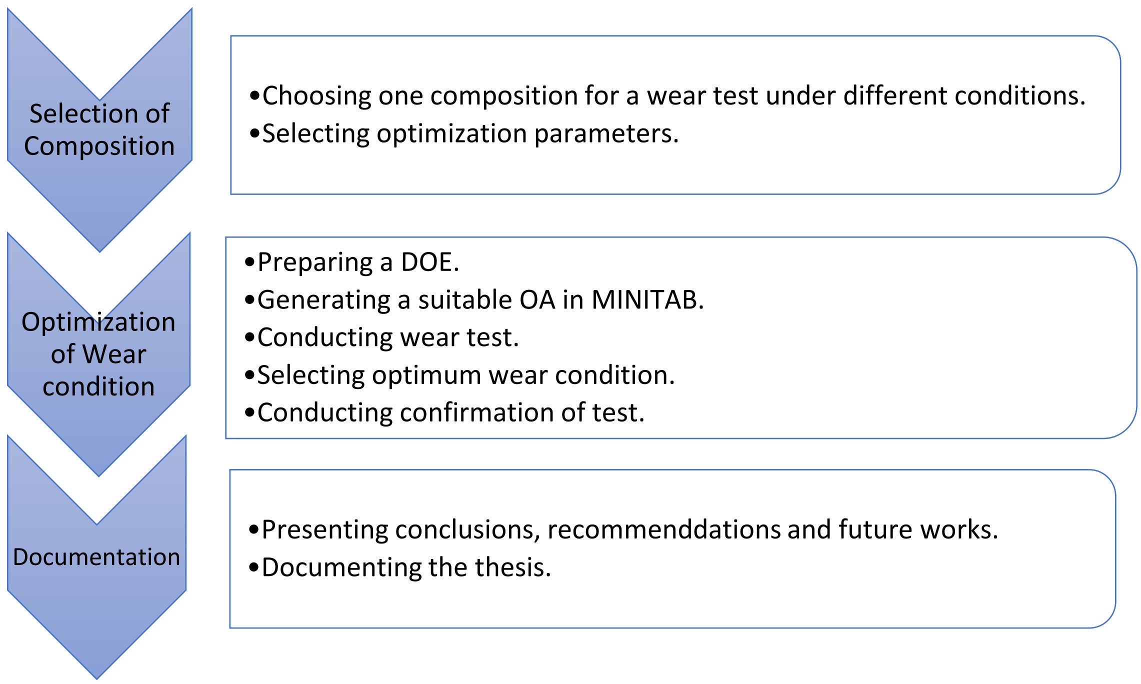

Figure 3.18. The workflow of the study: phase one (a) and phase two (b).

CHAPTER FOUR

4. RESULTS AND DISCUSSION

4.1. INTRODUCTION

In this chapter, different test results will be presented and will be discussed. The samples with their respective weight percentage are designated in Table 4.1. The sample code was given during the fabrication of the composite, in order of the melt.

Table 4. 1. Designation of the composite Samples.

Sample No	Sample code	Composition
Sample 1	M5	Al 90% + TiB210% + Gr 0%
Sample 2	M6	Al 88% + TiB2 10% + Gr 2%
Sample 3	M3	Al 86% + TiB2 10% + Gr 4%
Sample 4	M4	Al 84% + TiB2 10% + Gr 6%
Sample 5	M1	Al 82% + TiB2 10% + Gr 8%
Sample 6	M2	Al 80% + TiB2 10% + Gr 10%

4.2. MORPHOLOGICAL ANALYSIS

Figure 4.1. illustrates scanning electron microscope (SEM) images depicting the microscopic morphologies of samples of reinforcement particles. The samples basically revealed randomly distributed and equiaxed grains of titanium diboride (a) and graphite (b).

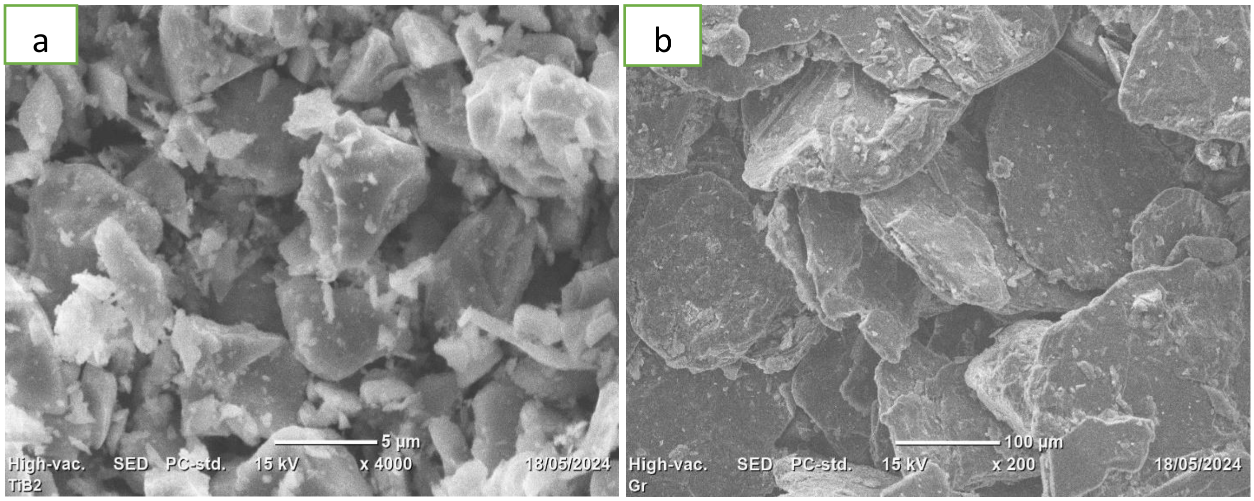

Figure 4. 1. SEM Micrograph image result for (a) TiB2 powder at 5um and 4000x magnification and (b) Gr powder at 100um and 200x magnification

With the help of the image processor, by randomly selecting a few numbers of grains from the SEM micrograph image, the mean grain size was measured to be about 4.398mirons for TiB_2. Similarly, For Graphite particles the average size of the grains was around 122 microns.

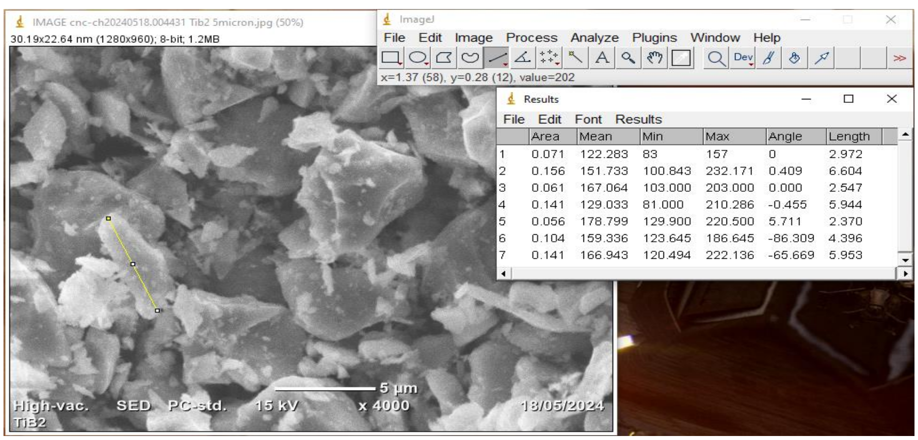

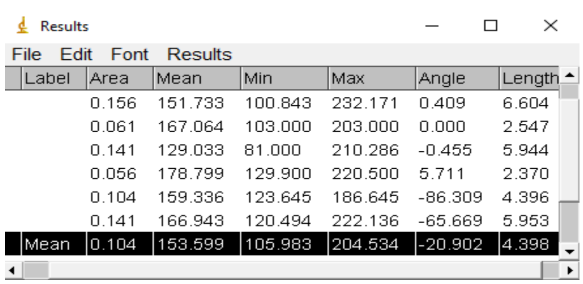

Results

Label	Area	Mean	Min	Max	Angle	Length
	0.156	151.733	100.843	232.171	0.409	6.604
	0.061	167.064	103.000	203.000	0.000	2.547
	0.141	129.033	81.000	210.286	-0.455	5.944
	0.056	178.799	129.900	220.500	5.711	2.370
	0.104	159.336	123.645	186.645	-86.309	4.396
	0.141	166.943	120.494	222.136	-65.669	5.953
Mean	0.104	153.599	105.983	204.534	-20.902	4.398

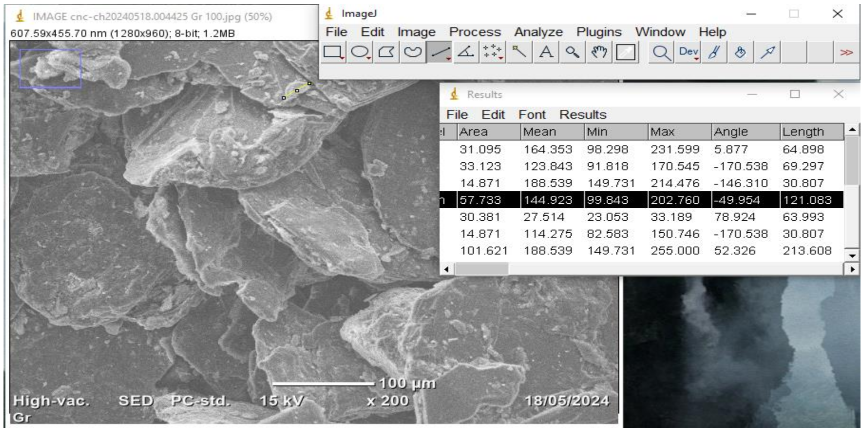

Figure 4. 2. Measurement of grain size of reinforcements using ImajeJ.

Granton al et. [90] described the form and shape of particles and explained Roundness and angularity are end members that describe the nature of the edges or corners of a particle. In addition to that, in terms of the packing of the particles, the porosity level can be lowered with Rhombohedral packing from a theoretical maximum of 47.64% porosity to a minimum of 25.95%.

Therefore, as shown in Figure 4.1., both particles' morphologies depict the arrangements of approximately equal particle sizes that can be considered as having a Rhombohedral packing. In terms of the surficial texture of the particle, Graphite can be characterized as bright and frosted. And, Titanium diboride can be described as a wetted type of surface texture.

C.S. Ramesh et al. [91] examined the Al6061-TiB2 in-situ composite's microstructure and observed that the addition of TiB_2 reinforcement has reduced the matrix alloy's grain size. The reduction is mostly due to TiB_2's capacity for grain refining, or nucleating more particularly.

4.3. MICROHARDNESS ANALYSIS

Micro-hardness testing is always important for the following applications:

- Microstructural hardness variations.
- Surface hardness
- Coating hardness
- Case depth
- Hardness of fragile or brittle metals

The results of the test are depicted in Table 4.2. As shown in the table, for every composite sample, multiple hardness test trials were conducted, and the average result was calculated. Figure 4.3. Shows the samples after the experiment.

Figure 4. 3. Samples after the Microhardness test was conducted.

Table 4. 2. Vickers' Hardness test results for the test specimens.

Sample No	Vickers hardness value, HV			Average Value
	Trial 1	Trial 2	Trial 3	
Sample 1	25.9	18.3	25.4	23.2
Sample 2	31.6	37.5	32.3	33.8
Sample 3	37.6	31.2	35.5	34.76
Sample 4	41.9	45.5	39.2	42.2
Sample 5	42.9	41.1	34.8	39.6
Sample 6	46.0	41.3	43.9	43.43

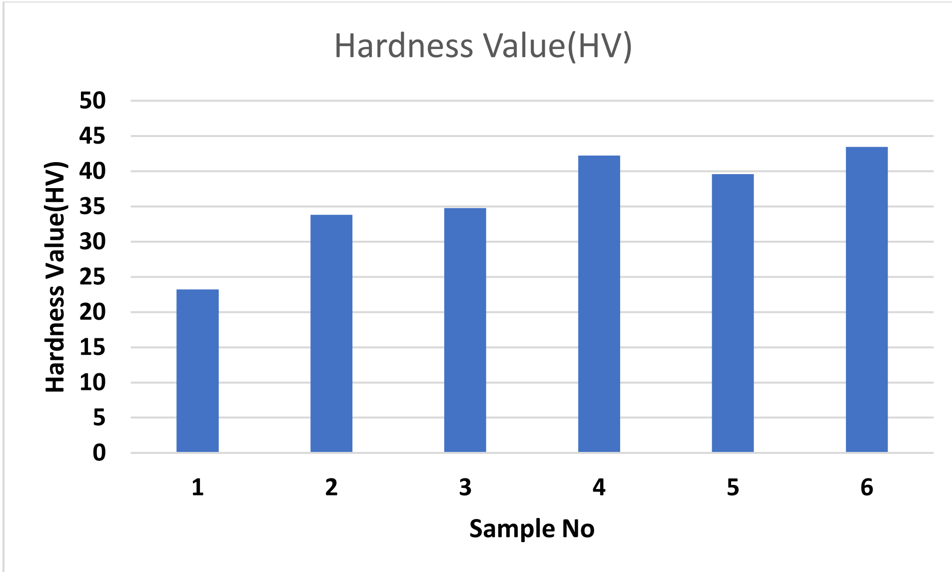

Figure 4. 4. Hardness values of the hybrid composite samples (Al 90% + $TiB_2$10% + Gr 0% to Al 90% + $TiB_2$10% + Gr 10%).

As shown in Figure 4.4., the hardness of the composite material is found to be higher than that of the unreinforced matrix metal, and a noticeable trend of increased hardness is observed as the volume fraction of graphite increases. This is due to the fact that these reinforcing particles increase the resistance to deformation when subjected to a load.

As shown in Table 4.2., The minimum and maximum hardness values from all of the samples of the composites were 18.3HV and 46HV respectively. In sample 1 (Al6061 + 10%TiB_2 + 0%Gr), by the addition of 2% of graphite reinforcement, the hardness value was drastically improved from 23.2 to 33.8HV. That is an increment of 45.6%. From Sample 2 to Sample 6, it can be visualized in the histogram that the hardness increases gradually. The Maximum hardness value for this experiment, 43.43HV, was obtained in 10% reinforcement composition in sample 6. From the base material (Sample 1), there is a total of 86.59% improvement in hardness.

As the Gr particle content increases, the composite gets harder, which enhances the composite's performance. The hardness of the composite will increase as a result of the hard material's imputed properties since ceramic particles have a higher hardness value than the soft aluminum metal matrix.

According to the results obtained from **Sivananthan et al.** [92] uniform stirring speed and optimal stirring time, of 10 minutes, enhance the particle distribution in the matrix material. A proper mixing of matrix and reinforcement materials during stir casting is essential to get a better property of a composite. As a result, between particles and the metal matrix, a good interfacial bonding will be created. Reinforcing particles enter the soft ductile metal matrix's lattice structure and hinder the mobility of atoms when there is a dislocation by providing greater resistance to plastic deformation. With increasing wt.% of reinforcements, grain boundary strength increases while dislocation density of atoms drops, giving strength to the matrix and hence the hardness of the composite increases. The hardness of the composite increases as the Gr particle content increases which will eventually improve the performance of the composite [93].

Therefore, it is reasonable to say the composites were able to resist localized damage during indentation by the diamond tip indented in the Vickers hardness test as a result of an increased percentage in weight of graphite particles. The microstructure of the samples falls in line with this conclusion.

4.4. WEAR ANALYSIS

WEIGHT LOSS:

The mass loss after conducting the pin-on-disc test was calculated by carefully weighing the samples before and after the test. The results are tabulated as follows.

Table 4. 3. Weight loss before and after the test for the samples.

Samples	Initial weight	Final weight	Weight loss
Sample 1	0.8039	0.7910	0.0129
Sample 2	1.0569	1.0476	0.0093
Sample 3	0.8885	0.8816	0.0069
Sample 4	1.1372	1.1325	0.0047
Sample 5	0.9574	0.9569	0.0025
Sample 6	0.9872	0.9851	0.0021

Figure 4. 5. Weight loss of the sample.

COEFFICIENT OF FRICTION:

The coefficient of friction is used with a variety of materials and circumstances, but it becomes more significant when friction is crucial to the material's ability to function as intended. The way the coefficient of friction test is set up might not accurately reflect how it would be used in practice. There could be variations in the size or form of the area of contact, the normal applied load, and the rotation speed, which could be significantly faster or slower. These circumstances cannot be replicated by the standard COF test. Certain materials' performance can be impacted by environmental variables like humidity and temperature. For this reason, lubrication is expected to be used in numerous applications.

The most evident and easily measured factor that can influence wear is the load or the contact stress. The normal load or contact stress magnitude is considerable because it increases the area of contact and the depth below the surface. The coefficient of friction is the ratio of the friction force which is a real-time value recorded in the tribometer test and the normal load applied to the pin, which is constant, 30N.

$$COF(\mu) = \frac{FF}{N} \quad (4.1)$$

Where FF is frictional force, and N is the normal load.

The Coefficient of Friction (COF) variation for each test specimen with time is shown in the Figure 4.6.

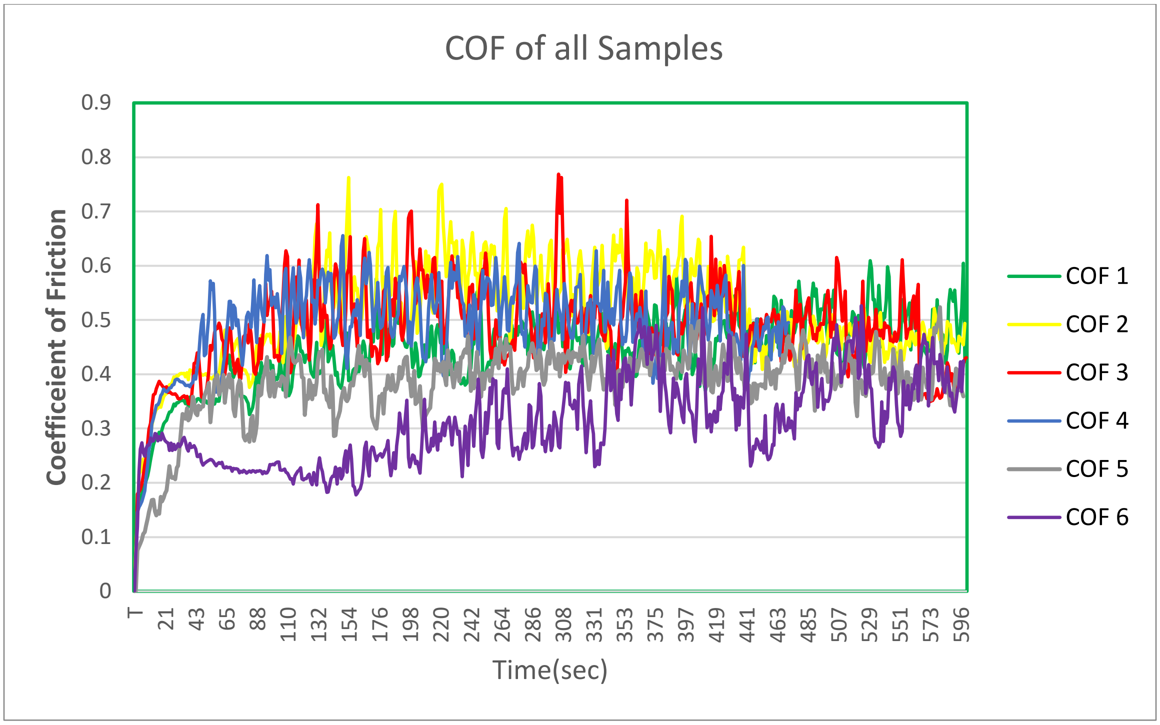

Figure 4. 6. Coefficient of friction for each sample with time.

The coefficient of friction of graphite-filled composites under a 30N load and 281m sliding distance is seen in Figure 4.6. The COF for the sample 5 (Al6061 82% + TiB2 10% + Gr 8%) and sample 6 (Al6061 82% + TiB2 10% + Gr 10%) has shown a significant decrease with the increased weight percentage of graphite.

In the case of 8% and 10% graphite-filled composites, Similar trends were seen in the COF variation, indicating that the composite reaches graphite saturation at 8% and above. The SEM images of the composites' surface validate these observations.

Table 4. 4. Coefficient of friction for each percentage of graphite.

	Gr percentage					
	0%	2%	4%	6%	8%	10%
Average Coefficient of Friction from the Test	0.54	0.50	0.49	0.48	0.39	0.38

The COF is significantly reduced when graphite filler is added to the glass fiber-reinforced composite in a relatable study. It is because graphite functions as a solid lubricant and it lowers the coefficient of friction. At a sliding distance of 281 m and a load of 30 N, the addition of 8% and 10% graphite to the Al6061-10%TiB_2 composite reduced the friction coefficient of the composite by 21.06%, from 0.54µ to 0.39µ and by 20.52% from 0.54µ to 0.38µ, respectively. It follows that the friction coefficient of the composite progressively decreases as the amount of graphite content increases.

The coefficient of friction plays a pivotal role in material selection for some applications. For some uses the friction coefficient is one of the key parts of the suitability of the material, such as for disc brakes and many other contacting parts.

FRICTION FORCE:

Figure 4. shows the frictional force against time of the POD experiment. Sample 1 and Sample 2 exhibit a higher number of friction forces. In the contrary, Sample 5 and Sample 6 show lower values of FF. Since the coefficient of friction and frictional force are directly proportional to each other, we notice a similar pattern in Figure 4. That shows COF plots.

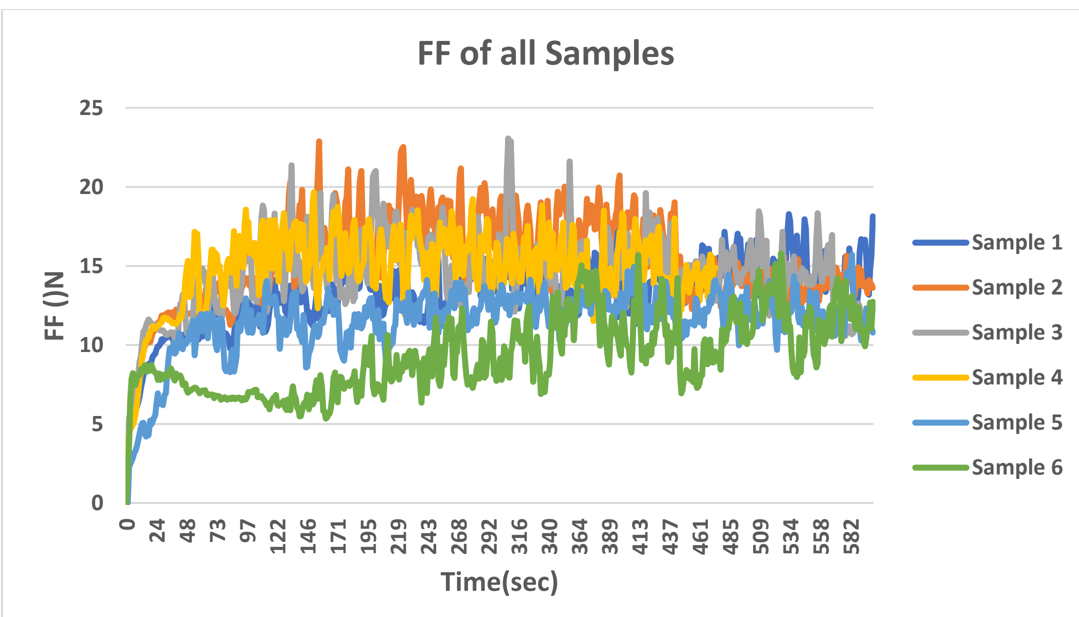

Figure 4. 7. Frictional force for all samples.

Therefore, these results also showed that the frictional force and coefficient of friction is lower for sample 5 (Al6061-10%TiB_2-8%Gr) and Sample 6 (Al6061-10% TiB_2-10%Gr).

WEAR RATE:

A commonly used equation to calculate the wear rate is **Archard et al.,1953** equation [94].

$$V_i = k_i F s \tag{4.2}$$

where F is the normal load, s the sliding distance, V_i the wear volume and k_i the specific wear rate coefficient. The Index i identifies the surface considered.

The k-value is given in m^3/Nm or m^2/N, sometimes in mm^3/Nm. From a design view, the wear displacement h is more convenient than V. With $h_i = V_i / A$, the contact pressure p=F/A where A is the area subjected to wear then:

$$h_i = k_i p s \tag{4.3}$$

The sliding distance, s, can be substituted by s=v.t where v is the average value for the slide rate and t the running time. Because the k-value similar to the friction coefficient depends on a lot of parameters and it is to be found experimentally.

But, other than this model, similar models are also being used to determine the wear rate. The following model is used for the wear rate comparison of the samples.

$$Wear\ rate = \frac{Weight\ loss}{Sliding\ distance} \tag{4.4}$$

$$Wear\ resistance = \frac{1}{Wear\ rate} \tag{4.5}$$

Wear volume loss is reported by this test method to eliminate confusion caused by changes in density, even though mass loss measurements can be used internally in laboratories to evaluate materials of equivalent densities. The appropriate care was taken to use and report the theoretical density value for the materials tested when calculating volume loss from measured mass loss.

The following equation should be used, according to ASTM-G99, to convert mass loss to volume loss..

$$volume\ loss, mm3 \ = \frac{mass\ loss, g}{density, g/cm3} \tag{4.6}$$

Now, by rearranging Eq. 4.3 and Eq. 4.5 we can calculate the wear rate (cm^3/m) as:

$$Wear\ rate = \frac{Mass\ loss, g}{Density, \frac{g}{cm3}\ x\ Sliding\ distance, m} \tag{4.7}$$

Density of the composites:

By applying Archimedes' principle to the density of base metal and reinforcements, we can determine the density of mono or hybrid composite materials. By applying the law of mixture to ascertain the occupied space of the reinforcements and matrix in the composite and their corresponding densities, the theoretical density of the composite samples has been determined [95].

Therefore, it can be computed using Eq. (4.7).

$$\rho_{th} = (\rho_{BM} * V_{BM}) + (\rho_{rein} * V_{rein})^n \tag{4.8}$$

Where, V_{BM} and V_{rein} are percent contribution in the composite, ρ_{BM} and ρ_{rein} are the base metal and reinforcement densities respectively. And, n represents the number of reinforcements.

To determine the wear rate of each specimen, we now calculate the theoretical densities, which are concurrent with experimental results, for each specimen.

For sample 1:

$$\rho_{th} = (\rho_{Al} * V_{Al}) + (\rho_{TiB2} * V_{TiB2})$$

$$\rho_{th} = (2.71 * 0.9) + (4.52 * 0.1) = \underline{\underline{2.891 g/cm^3}}$$

For sample 2:

$$\rho_{th} = (\rho_{Al} * V_{Al}) + (\rho_{TiB2} * V_{TiB2}) + (\rho_{Gr} * V_{Gr})$$

$$\rho_{th} = (2.71 * 0.88) + (4.52 * 0.1) + (2.26 * 0.02) = \underline{\underline{2.882 g/cm^3}}$$

For sample 3:

$$\rho_{th} = (\rho_{Al} * V_{Al}) + (\rho_{TiB2} * V_{TiB2}) + (\rho_{Gr} * V_{Gr})$$

$$\rho_{th} = (2.71 * 0.86) + (4.52 * 0.1) + (2.26 * 0.04) = \underline{\underline{2.873 g/cm^3}}$$

For sample 4:

$$\rho_{th} = (\rho_{Al} * V_{Al}) + (\rho_{TiB2} * V_{TiB2}) + (\rho_{Gr} * V_{Gr})$$

$$\rho_{th} = (2.71 * 0.84) + (4.52 * 0.1) + (2.26 * 0.06) = \underline{\underline{2.864 g/cm^3}}$$

For sample 5:

$$\rho_{th} = (\rho_{Al} * V_{Al}) + (\rho_{TiB2} * V_{TiB2}) + (\rho_{Gr} * V_{Gr})$$

$$\rho_{th} = (2.71 * 0.82) + (4.52 * 0.1) + (2.26 * 0.08) = \underline{\underline{2.855 g/cm^3}}$$

For sample 6:

$$\rho_{th} = (\rho_{Al} * V_{Al}) + (\rho_{TiB2} * V_{TiB2}) + (\rho_{Gr} * V_{Gr})$$

$$\rho_{th} = (2.71 * 0.80) + (4.52 * 0.1) + (2.26 * 0.1) = \underline{\underline{2.846 g/cm^3}}$$

The summary for the calculated densities of each sample is shown in Table 4.5.

Table 4. 5. Density of the composites.

Sample No	Density, ρ, (g/cm^3)
Sample 1	2.891
Sample 2	2.882
Sample 3	2.873
Sample 4	2.864
Sample 5	2.855
Sample 6	2.846

By doing the above simple calculations, we can find the volume loss and the wear rate for each sample. The sliding distance of the wear track at a speed of 0.471m/s and applied load of 30N for 10 minutes is found to be 281m. The results are put in Table 4.6.

Table 4. 6. Wear rate and Volume loss of the specimens.

Sample No	Initial Weight (g)	Final Weight (g)	Weight Loss (g)	Volume loss (g/cm^3)	Wear Rate (mm^3/N-m)
Sample 1	0.8039	0.7890	0.0149	0.005153	0.000611
Sample 2	1.0569	1.0476	0.0093	0.003226	0.000382
Sample 3	0.8885	0.8816	0.0069	0.002401	0.000284
Sample 4	1.1372	1.1325	0.0047	0.001641	0.000194
Sample 5	0.9574	0.9569	0.0025	0.000875	0.000103
Sample 6	0.9872	0.9851	0.0021	0.000737	0.000087

A transition condition from mild to severe wear has been linked by a few authors to a wear rate in the range of 10^{-6} to 10^{-4}. Smooth surfaces and wear rates <10^{-6} mm^3/N-m are related to a small regime; microfractures, grooves, and wear rates >10^{-6} are associated with a severe regime. Figure 4.8. displays wear curve diagrams for composite specimens with 0, 2, 4, 6, 8, and 10 percent graphite particle content.

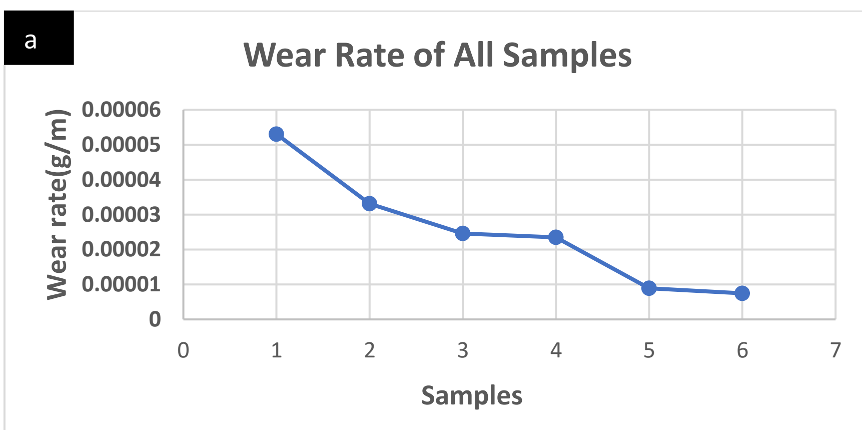

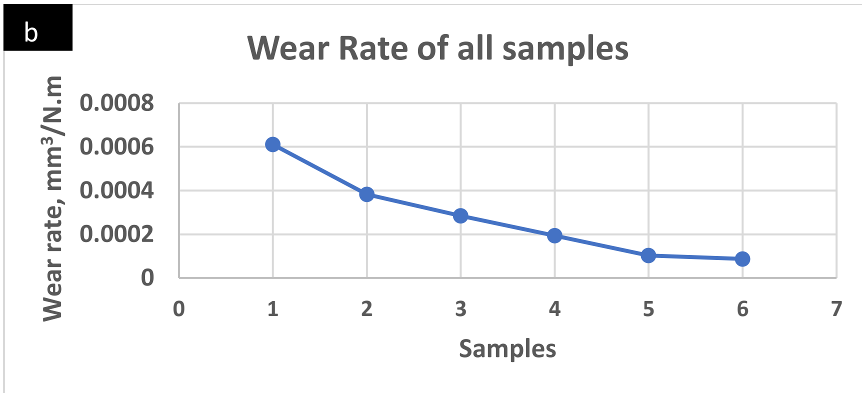

Figure 4. 8. Wear rate of all samples in (a) g/m and (b) mm^3/N-m

As the amount of reinforcement particles in the composites increases, they also improve their wear resistance. Ma et al. (1996) [96] observed a similar wear behavior trend. This is caused by the hardness of the titanium diboride particles during sliding motion and the lubricating coating that is created by the graphite particles.

As it is observed in the Figure 4.8., the wear rate of composites reinforced with 10 percent TiB_2 and 8 percent graphite has declined nearly Seven times than from that of the base material (10 percent TiB_2 with no graphite) (sample 1) or improved by 83.18% and almost 4 times than the Al6061 reinforced with 10% TiB_2 and 2% graphite particles (sample 2). The wear rate for Sample 6 showed a reduction of 85.77% compared to sample 1.

All of the compositions' wear rates initially decreased as the sliding distance increased and then they became constant and ceased to increase after that. Owing to the high hardness of 10%TiB_2 + 8% and 10 % Gr reinforcements, sample 5 and sample 6 showed the lowest wear rate.

4.5. SEM MICROSTRUCTURE ANALYSIS

A liquid alloy's microstructure can separate into up to three different zones as it solidifies in a mold. The chill zone, where the fine, equiaxed grains with a primarily random crystallographic orientation form, is in contact with the mold wall. The chilling that happens when the liquid first comes into touch with the cold wall is what drives the nucleation of grains in this zone, which can happen on the wall directly or as a result of the melt's heterogeneities. By heating the mold, the zone can be eliminated. The columnar zone is created by the grains becoming longer as the casting solidifies closer to its center. Certain grains have their preferred development direction in the chill zone more nearly antiparallel to the heat flow; these grains grow at a lower rate of supercooling and gain a preferred crystallographic orientation in the columnar zone by surpassing other grains at the liquid-solid interface [97].

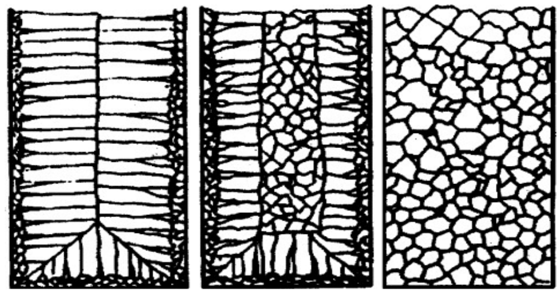

Figure 4.9. Different Microstructure zones of a liquid alloy [97].

H.Q. Wang et al. [98] studied Al6061 casting rod structure and revealed the casting rod's chilled surface area as well as the center's grain form during deep corrosion. The precipitates were present both inside and outside the grain of the base structure, which included a white, light α-Al phase. Both the grain's center and surface have the same equiaxed shape.

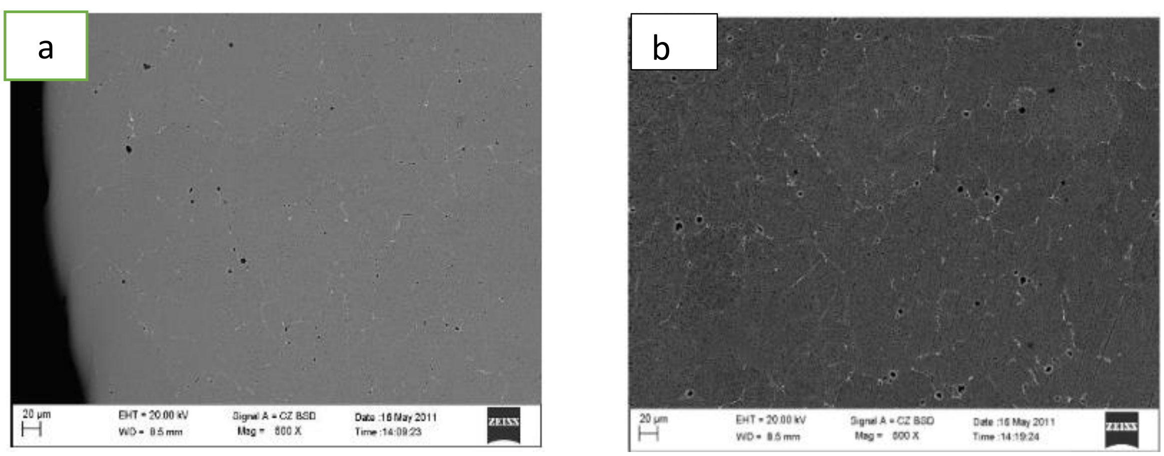

Figure 4. 9. Al6061 casting rod chilled surface (a) and the grain shape in the center after deep corrosion (b)

Figure 4.10. shows SEM micrograph images of all of the samples. Good quality images were chosen for a clearer view of the microstructure with different micrograph magnifications ranging from 500x to 1000x and 5µm to 100µm.

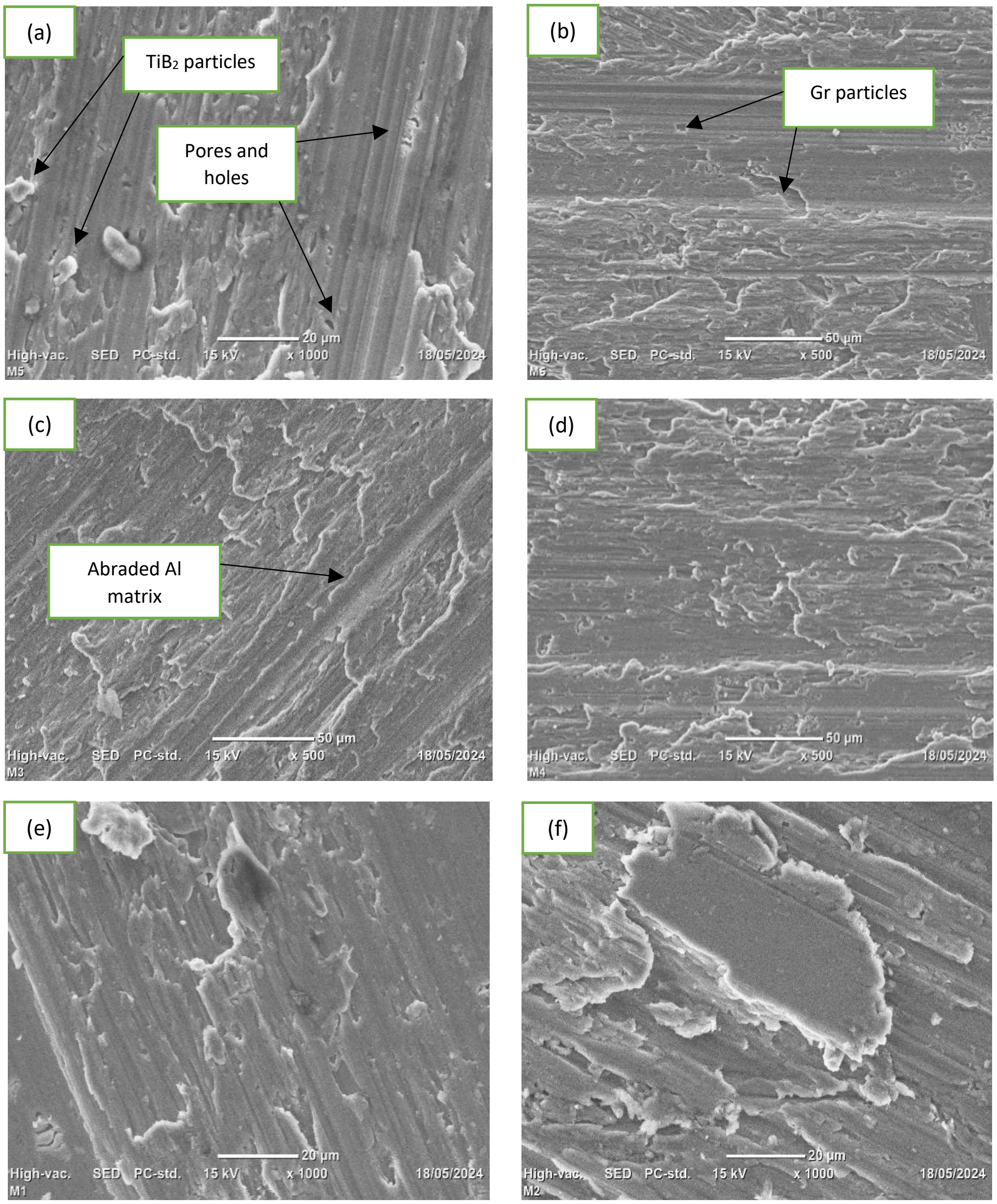

Figure 4. 10. SEM micrograph images of (a) Sample 1(Al6061 + 10%TiB2 + 0%Gr) (b) Sample 2 (Al6061 + 10%TiB2 + 2%Gr) (c) Sample 3(Al6061 + 10%TiB2 + 4%Gr) (d) Sample 4(Al6061 + 10%TiB2 + 6%Gr) (e) Sample 5(Al6061 + 10%TiB2 + 8%Gr) (f) and Sample 6 (Al6061 + 10%TiB2 + 10%Gr)

As illustrated in Figure 4.10., In Sample 5 (Al6061 + 10%TiB2 + 8%Gr) and Sample 6 (Al6061 + 10%TiB2 + 10%Gr), TiB_2 and Gr particles are more densely distributed in the MMC. This is due to a higher percentage of composition of the reinforcements in the composite.

Although the precise mechanisms are outside the scope of this chapter, break-up is an important occurrence to note; microstructures that show scattered nucleation may have a completely distinct origin that is not susceptible to any nucleation investigation.

The microstructure of the composites formed by the reinforcing particles, which were generally twinned and only a few µm in size. There were no foreign impurity atoms seen at the contact according to the SEM.

Porosity:

It is usually the case that reinforcing metallic matrices with ceramics causes voids in the microstructure due to ceramic aggregation, a considerable difference in surface energy between ceramics and metals, and arbitrary shape of the ceramics with sharp edges. Reinforcement may increase the percentage of porosity in an aluminum matrix composite for a variety of reasons. The reinforcing particles might act as gas bubble nucleation sites during the manufacturing process, which would increase porosity. This is one explanation for the porosity increase. Another reason is that adding reinforcement increases the viscosity of the molten metal matrix, which would make it difficult for gas bubbles to escape during solidification and lead to closed voids in the final product. Additionally, dispersion caused by reinforcing particles in molten aluminum metal may result in gas bubble entrapment [99]. Eventually, these gaps will have a detrimental effect on the mechanical, thermal, and even operational aspects of composites. Because it regulates the porosity in composites, the size of the reinforcing particles is also a critical factor in determining the wear and fracture behavior of metal matrix composites. [100].

By using ImageJ, the porosity level was measured with the help of the Threshold tool. The techniques and tools used for measuring particle size and porosity level are shown as a screenshot in Appendix IV. For sample 1, 5.681% of the porosity level was measured. By following similar steps, the porosity level for sample 2 is 6.192%, 6.86% for sample 3, 7.945% for sample 4, 9.441% for sample 5, and 10.164% for sample 6.

To compare the outcomes with similar studies, Cole et al. 2022 [101] also used this software for quantifying cortical pore morphometry on bone images and it delivered the desired output.

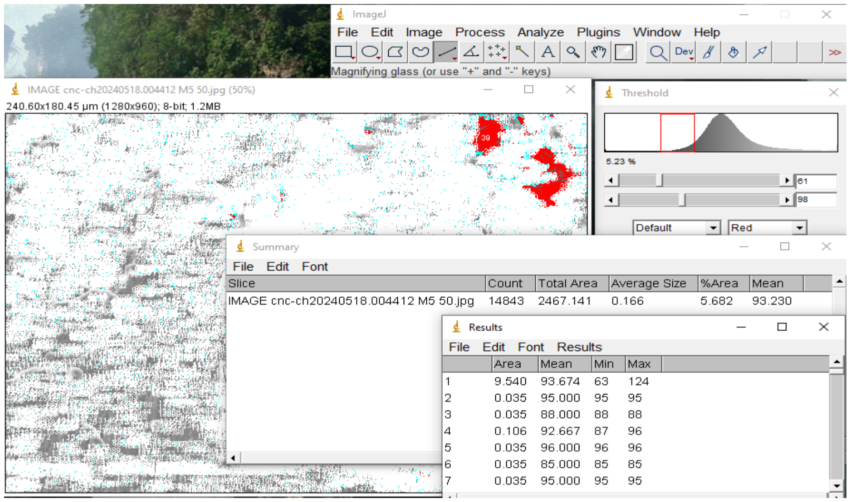

Figure 4. 11. Image J results for porosity examination of samples.

4.6. OPTIMIZATION OF WEAR PROCESS PARAMETERS

This section is part of phase two of the study. After completing all the examinations and tests on all samples of different compositions, the result of the test was analyzed; and also compared to results and conclusions of similar researchers. The selection of a sample for optimization of wear condition is explained in the next sub-section.

4.6.1. SELECTION OF ONE COMPOSITION OF THE COMPOSITES FOR OPTIMIZATION OF WEAR CONDITION

For the wear performance of a hybrid composite material to be better, the proportion of reinforcement should be carefully selected to increase wear resistance. If there is an excessive reinforcement in the material, as a result, the goal of reinforcement will be defeated. Comparably, A component with too much reinforcing will become less ductile and lose its toughness other important characteristics that are desired in composites. The following literature among many others has also shown similar conclusions.

Manoj et.al [102] demonstrated a 79.54% improvement in the tensile strength of composites reinforced with titanium diboride (TiB_2). Nonetheless, elongation decreased by 45.47% in comparison to the matrix material of Al alloy.

Manohar et al. [103] examined the mechanical properties of Al7075/SiC/8%Gr ; the findings showed that the hybrid composite with an optimal weight percentage of 8% graphite had significantly improved mechanical properties.

According to Sharma et al., [104] study on the wear behavior of the Al6101/Gr composite, graphite's brittleness as a reinforcement causes the brittleness in the aluminum matrix composites to increase, thereby reducing their ductility. The flexural strength of cast Al6101 metal matrix composites is shown in Figure 4.12. It demonstrates that when the percentage of graphite in Al6101 increased, the composites' flexural strength decreased. The creation of a small lubricating coating on the tribosurface as a result of the higher graphite reinforcement content in the Al6101 metal matrix was the reason for this decrease in wear rate. As a result, their mechanical properties were degraded by an increase in porosity and cracks caused by an increased graphite content.

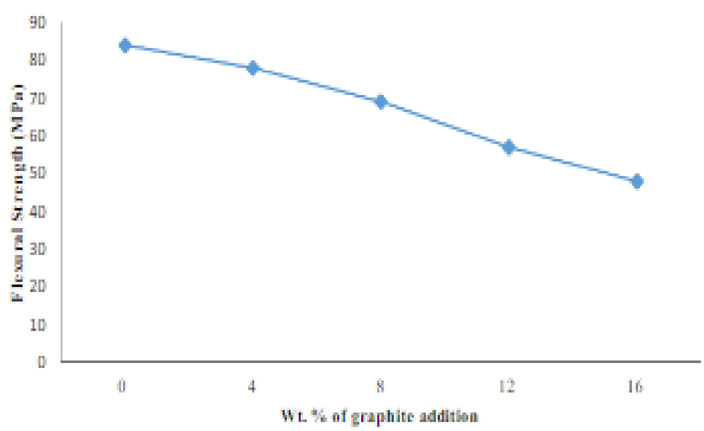

Figure 4. 12. Flexural strength of Al6101 vs Weight percentage of graphite reinforcements [101].

Along with several other suggestions from the literature, the sample that was selected for further parametric optimization of wear processes was sample 5, Al6060 + 10TiB_2 + 8% Gr.

Based on ASTM-G99 standards for pin-on-disk wear test, test samples from sample 5 were prepared and the standard procedures were followed in conducting the optimization process of the designed experimental runs.

Mass Loss:

Similarly to the first experiments, the mass of the specimens before and after each experimental run was weighed and the mass loss after wear was recorded carefully and presented in Table 4.7.

Table 4. 7. Experimental results for the mass loss of L9 OA runs.

Exp'tal Run	Load (N)	Speed (RPM)	Time (Min)	Weight Before(g)	Weight After(g)	Total Weight Loss(g)
1	20	200	5	0.9236	0.9229	0.0007
2	20	300	10	1.0021	0.9995	0.0026
3	20	400	15	0.9945	0.9512	0.0433
4	30	200	10	0.9229	0.9221	0.0008
5	30	300	15	0.9995	0.9950	0.0045
6	30	400	5	0.9512	0.9500	0.0012
7	40	200	15	0.9221	0.9198	0.0022
8	40	300	5	0.9950	0.9888	0.0062
9	40	400	10	0.9500	0.9465	0.0035

COF:

An important parameter that is examined together with assessing the materials' resistance to wear is the coefficient of friction. Figure 4.13. shows the variation of the coefficient of friction (COF) for every experimental run with time. The mean coefficient of friction collected from the experiment is shown in Table 4.8.

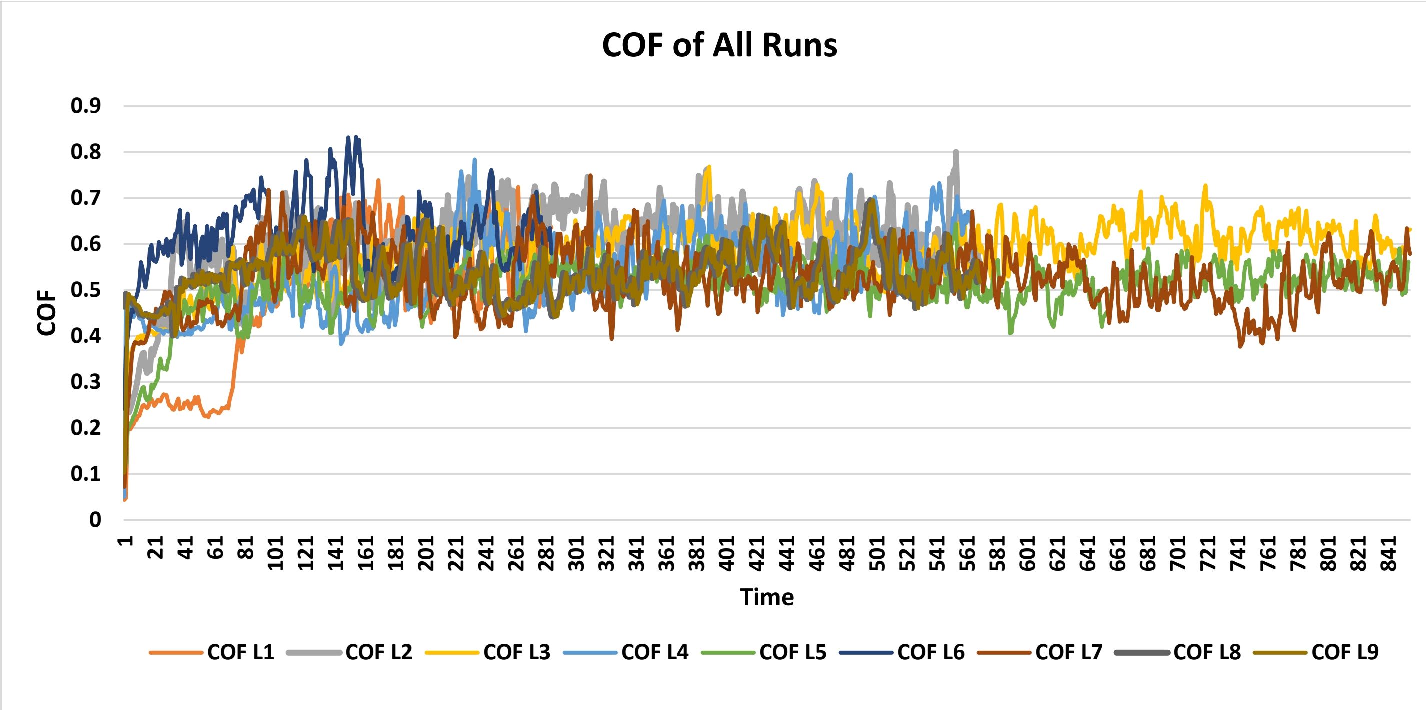

Figure 4. 13. COF for L9 OA experiments.

Table 4. 8. Coefficient of friction for each experimental run.

	Experimental Runs								
	1	2	3	4	5	6	7	8	9
Average COF	0.44	0.51	0.50	0.49	0.49	0.55	0.45	0.46	0.48

WEAR RATE:

For the analysis of the wear rate of the selected specimen, the experiment was conducted using a pin-on-disc tribometer with the respective combination of load, speed, and time according to the design for each experiment run. Therefore, each test had a separate set of parameters. The pin specimen had undergone surface erosion as a result of the friction that developed between the pin and disc during the test. The main objective of the test was to calculate the specimens' mass loss following each test.

Now, as it was discussed in the previous section (4.4), The volume reduction can be calculated as the mass reduction value divided by the density of each pin material. However, the pin composite material selected for the experiment has a calculated density and it is similar for all experimental runs. Therefore, it is possible to use Equation 3.3. for the determination of the wear rate for each run by doing a simple calculation.

$$Wear\ rate = \frac{Weight\ loss}{Sliding\ distance} \tag{4.3}$$

Table 4. 9. The wear rate of all experimental runs.

Exp'tal Run	Mass loss (g)	Sliding distance (m)	Wear Rate 10^{-4}(g/m)
1	0.0007	94	0.0744
2	0.0026	281.6	0.0923
3	0.0433	565.5	0.7656
4	0.0008	188.5	0.0424
5	0.0045	424	0.0106
6	0.0012	188.5	0.0636
7	0.0022	282	0.0780
8	0.0062	141.4	0.4384
9	0.0035	377	0.0928

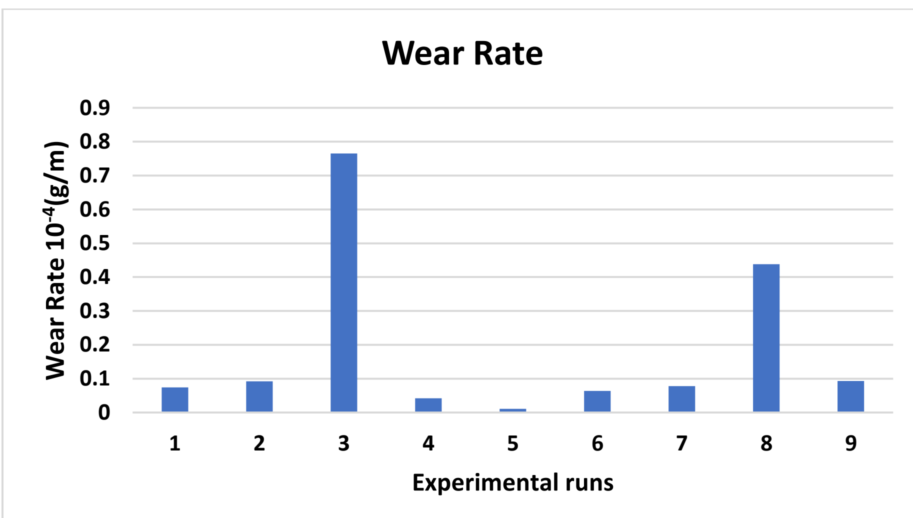

Figure 4. 14. Wear rate for all experimental run.

4.6.2. TAGUCHI ANALYSIS FOR COF AND WEAR

The goal of the wear test was to find out how process parameters impact the COF and Wear Rate. The L9 Orthogonal array was selected and tests were performed according to the design. The results of the experimental for COF, the Wear rate, and the S/N ratios of COF and Wear rates are tabulated in Table 4.10.

Table 4. 10. S/N Ratio response table for L9 OA experimental tests.

Experimental Run	Load (N)	Speed (RPM)	Time (Min)	COF	S/N ratio for COF	Wear 10^{-4} (g/m)	S/N Ratio for Wear
1	20	200	5	0.44	10.0188	0.0744	22.5685
2	20	300	10	0.51	8.7189	0.0923	20.6960
3	20	400	15	0.50	3.7875	0.7656	2.3200
4	30	200	10	0.49	9.1740	0.0424	27.4527
5	30	300	15	0.49	9.2043	0.0106	39.4939
6	30	400	5	0.55	8.1454	0.0636	23.9309
7	40	200	15	0.45	9.8175	0.0780	22.1581
8	40	300	5	0.46	6.9487	0.4384	7.1626
9	40	400	10	0.48	9.2261	0.0928	20.6490

4.6.3. ANALYSIS AND DISCUSSION OF THE RESULT OF COF

4.6.2.1. S/N Ratio of COF

After employing the Taguchi design and conducting the experiments according to L9 orthogonal array, to verify the sliding parameter, the response table plotted alongside the corresponding S/N graph is shown in Figure 4.15.

To determine the S/N values for this investigation, given that the lowest coefficient of friction is preferred in terms of material's friction and wear characteristics, Taguchi analysis employed the following formula, which corresponds to the "smaller is better" principle.

$$\mathbf{S/N = -10 \log_{10}[1/n(SUM(Y_i^2))]} \qquad (4.9)$$

Where, Y_i= measured Wear rates or COF and n is the number of tests performed.

Table 4. 11. Response table for Coefficient of friction.

	S/N ratio Response			Mean Response		
Level	Load (N)	Speed (RPM)	Time (Min)	Load (N)	Speed (RPM)	Time (Min)
1	7.508	9.670	8.371	0.3970	0.2625	0.3377
2	8.841	8.291	9.040	0.2744	0.3336	0.2846
3	8.664	7.053	7.603	0.3332	0.4087	0.3824
Delta	1.333	2.617	1.437	0.1226	0.1462	0.0978
Rank	3	1	2	2	1	3

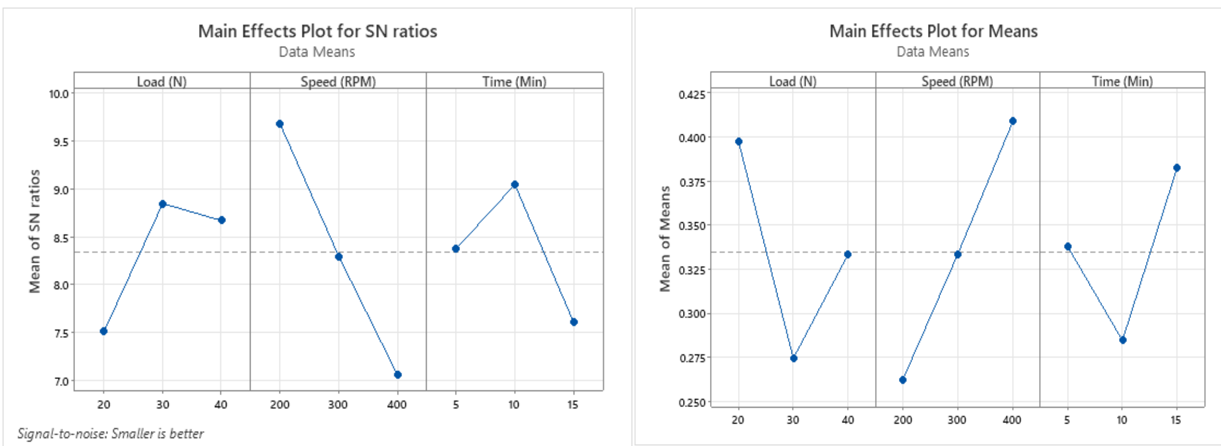

Figure 4. 15. Response graphs of Main effect plots for Coefficient of Friction.

4.6.2.2. Selection of optimal level for COF

The S/N response's delta ranks are used to determine the optimal values. The delta statistics were calculated as the difference between each factor's highest and lowest average value. The biggest value of delta, which was assigned the first rank, is the factor that most significantly affects the coefficient of friction.

According to the ranks of the parameters, for COF, the disk rotation Speed (RPM) has a mean delta value of 0.1462 and is ranked highest followed by Load with a delta value of 0.1226 and time with a delta value of 0.0978.

The best possible combination of the parameters in the signal-to-noise ratio is identified by the maximum point on each level. As it is shown in the figure, the best combinations are:

A2B1C2

Therefore, the most effective combinations of process parameters for COF are 200RPM disk speed with a load of 30N and for 10 minutes.

4.6.2.3. ANOVA for COF

The process parameter that primarily influences the performance attributes is provided by ANOVA. Table 4.12. provides a summary of the analysis of variance results.

Table 4. 12. Analysis of variance for COF.

Source	Degree of Freedom	Sum of squares	Mean squares	% Contribution
Load (N)	2	2.80112	1.40056	16.6
Speed (RPM)	2	1.11018	0.55509	33.4
Time (Min)	2	0.08271	0.04135	8.71
Residual Error	2	0.55725	0.27863	
Total	8	4.55126		100

As shown from the signal-to-noise ratio plots, it was determined that speed has the most influence from the process parameters. However, with the help of ANOVA analysis, the percentage contribution was also calculated.

The speed of the rotating disk in the experiment has a 33% contribution to the process and to the optimal parametric setting. Following that, Load has a 16% contribution and lastly, time has the minimum percentage contribution with only 8.71%.

Regression Equation:

COF = 0.4439 - 0.00100 Load (N) + 0.000250 Speed (RPM) - 0.00033 Time (Min) (4.10)

The Coefficient of determination, R square is 82.64 % which can be considered acceptable but it is always better if it is about 90%. This suggests that the model can predict the response values at any combination of parameter values.

4.6.4. ANALYSIS AND DISCUSSION OF THE RESULT OF WEAR

4.6.4.1. S/N Ratio of Wear

Based on the principle of reducing the noise factors for wear rate, the S/N ratios for smaller-the-better conditions were identified.

The signal-to-noise ratio responses, wear vs. load, speed, and time collected from Taguchi analysis, similar to the COF analysis section, are presented in Table 4.12.

Table 4. 13. Response table for Wear rate.

	S/N ratio Response			Mean Response		
Level	Load (N)	Speed (RPM)	Time (Min)	Load (N)	Speed (RPM)	Time (Min)
1	15.19	**24.06**	17.89	**0.31077**	0.06493	0.19213
2	**30.29**	22.45	**22.93**	0.03887	0.18043	0.07583
3	16.66	15.63	21.32	0.20307	**0.30733**	**0.28473**
Delta	15.10	8.43	5.05	0.27190	0.24240	0.20890
Rank	1	2	3	1	2	3

Measurement quality is crucial for improving signals while accounting for uncontrollable factors, or for lowering response noise. that reacts with ideal qualities in the anticipated composite product.

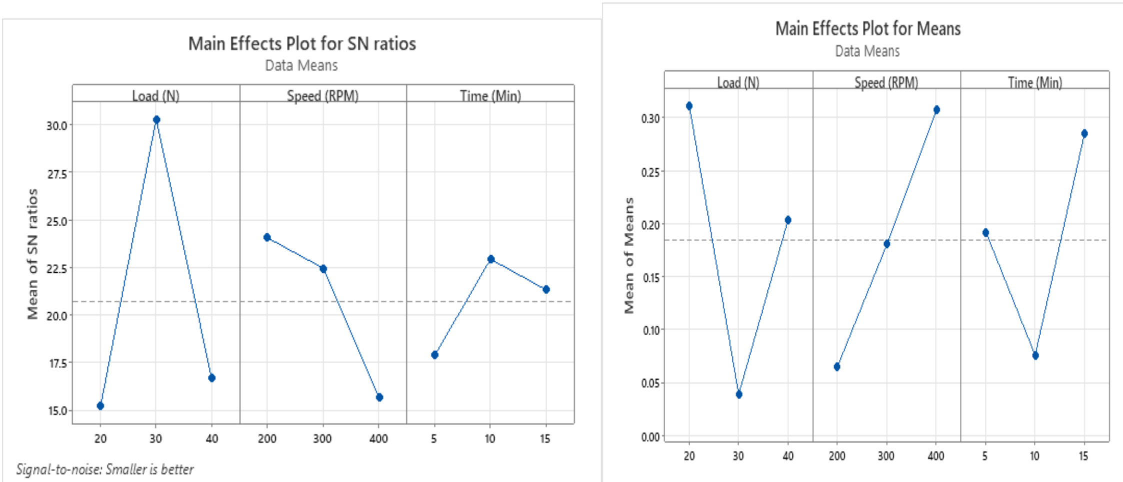

Figure 4. 16. Response graphs of Main effect plots for Wear.

4.6.4.2. Selection of optimal levels for Wear

In this experimental analysis, the main effect plot in Figure 4.16. was used to estimate the mean Wear rate with optimal parameter conditions. The optimum parametric condition is achieved when the combination of factors is:

A2B1C2

That tells us that the optimal wear condition of this experiment is obtained at a Load of 30N, at a Speed of 200RPM, and for 10 minutes.

The delta value, which is the difference between the minimum and highest S/N ratios of the control factor, is used to determine which control factor has the greatest influence. From Table 4.13., it is shown that the delta value for the control factors is 15.1 for Load and has ranked first, followed by an 8.43 delta value for Speed and lastly Time with a 5.05 delta value. Therefore, it is evident that the Load has more influence on wear than any other control process parameter.

4.6.4.3. ANOVA for Wear

After analyzing the impacts of control parameters (Load, Speed, and Time) on wear rate, ANOVA yielded various statistical results such as the percent contribution, sum of squares, residual error, and the degree of freedom as shown in Table 4.14.

Table 4. 14. ANOVA for Wear rate.

Source	Degree of Freedom	Sum of squares	Mean squares	% Contribution
Load (N)	2	416.01	208.01	44.44
Speed (RPM)	2	120.07	60.04	12.8
Time (Min)	2	39.85	19.93	4.2
Residual Error	2	360.01	180.01	
Total	8	935.95		100

According to the ANOVA results, the most important parameter influencing the wear rate was found to be the load with a 44.44% contribution. Following that, speed has 12.8% contribution and time has a minimum influence of 4.2% contribution. ANOVA was able to verify the results of the main effect graphs of wear in Figure 4.16.

By using the regression equation, wear prediction that account for the different process parameters were obtained. For that, a linear regression analysis was generated and a regression equation is presented below.

Regression Equation:

$$\textbf{Wear Rate } 10^{-4}(\text{g/m}) = -0.110 - 0.0054 \text{ Load (N)} + 0.00121 \text{ Speed (RPM)} + 0.0093 \text{ Time (Min)} \quad (4.11)$$

The Coefficient of determination, R square is 81.86 % which can be considered acceptable but it is always better if it becomes about 95%. This suggests that the model can accurately predict response values for any value of the parameter.

4.6.5. CONFIRMATION OF EXPERIMENTS

This step of the study can be treated as simply another step to do as part of an optimization process. A brief confirmation experiment might be adequate in certain situations, but more work will be required in others to ensure that the results are more widely applicable and to accurately validate the information learnt from the previous trials. Long-lasting process improvements brought forth by optimal factor combinations are reinforced by confirmation. A single example of a successful outcome may not be enough; the ability to consistently accomplish the desired goals raises the possibility that the outcomes may last for a longer period of time.

The optimal parameter values were 30N of load, 200RPM speed, and for 10 minutes. The COF and the wear confirmation test are shown in Table 4.15.

Similar to the wear analysis done in the previous section, the COF and Wear rate for this confirmation test were determined according to the collected data from the pin-on-disc test and by using Eq 4.4. whereas, the predicted values were determined based on the equations Eq 4.10 and Eq 4.11. The raw data from the test is shown in APPENDIX VII.

For the confirmation test, the weight loss = 0.9516 – 0.9505 = 0.0011g. Therefore, the wear rate for a 188.5m sliding distance will be 0.0583×10^{-4} g/m.

The experimental values and predicted values are typically fairly close to one another. A statistical analysis can only be considered reliable if the error values are less than 20% [102].

Table 4.15. Confirmation test for COF and Wear.

Levels	COF			Wear		
	Predicted	Experimental	Error (%)	Predicted	Experimental	Error (%)
Opt. Level A1B1C2	0.4606	0.414	**10.11%**	0.063	0.0583	**7.37%**

This result demonstrates the smallest variance between the experimented values and the expected values. The wear rate and the coefficient of friction has shown a 10.11% and 7.37%, respectively, deviation from the predicted value of the Taguchi analysis, which can be considered acceptable.

CHAPTER FIVE

5. CONCLUSION, RECOMMENDATION, AND FUTURE WORK

5.1. CONCLUSION

In this thesis work, the influence of graphite particles in the aluminum 6061 and a constant 10% titanium diboride particles on its wear behavior was studied in the first phase of the study. In the second phase, the optimization of wear process parameters was conducted on a selected composite sample. Based on the foregoing discussion of Al6061 and Titanium diboride composite and its relative comparison with the addition of varying percentages of Graphite particles, and based on the optimization of the control factors on a pin on disk wear tests, the following conclusions can be drawn.

- The hardness of the composites significantly enhances as a result of the addition of the graphite particles because of their lubricating characteristics.
- Wear rate rapidly decreases as the graphite particle is introduced into the hybrid composite and then keeps decreasing gradually as the graphite percentage increases with an interval of 2%.
- Wear behavior gives a good correlation with hardness. The relationship between wear rate and mechanical properties validates Archard's equation. As the hardness of the composite increases due to the ceramic particles with good lubrication behavior, wear tends to decline.
- The optimum parametric condition for COF and wear rate was achieved when the combination of factors is at a Load of 30N, at a Speed of 200RPM, and for 10 minutes with confirmation of test also supporting the conclusion with a 10.11% and 7.37%, respectively, deviation from the predicted value.
- According to the results of statistical analysis, it is observed that the load has the most influence on wear, as it increases wear rate also increases, and the disk speed parameter is more significant for the coefficient of friction, COF increases with lower disk speed.

5.2. RECOMMENDATION

Based on the results and conclusions found from this study, the following recommendations were made:

- ✓ It can be suggested that the hybrid composite (Al6061, 10TiB_2, and Gr) can be vastly used as an appropriate substitute for materials used in the manufacturing of automotive and aircraft parts because it exhibits significant improvements in hardness and other desired properties than the conventional aluminum alloy.
- ✓ During a wear test or a real-life application of the composites, it is beyond vital to take into consideration that the load condition, the speed, and the amount of time heavily influence the wear characteristics of the composite and the recommended combinations of parameters need to be given attention.
- ✓ In this study, a few mechanical and tribological properties were studied and characterized. Other mechanical property tests, like as, tensile and impact tests, can be employed for further investigations and interesting findings about these aluminum-based MMCs.

5.3. FUTURE WORK

In this study, the wear behavior of A16061 metal matrix reinforced with 10% titanium diboride and varying composition of graphite using the stir casting method was studied. Optimal stir casting parameters were utilized according to the review of literature and tests were performed to explore the hybrid metal matrix composite. However, lots of other areas can be studied in the future based on these hybrid composite combinations. The following areas can be considered:

- The behavior of this hybrid metal matrix with other fabrication methods like powder metallurgy can be studied.
- The potential of these composites within a specific application and under different conditions in the aerospace and aircraft industry can be studied using analytical and finite element analysis methods.
- Additional research works on the hybrid composite's mechanical properties will help to explore further about the material's characteristics.

REFERENCES

1. R. Gukendrana, M. Sambathkumara, K. S. K. Sasikumara, D. K. Karupannasamya 'Effect of Silicon Carbide and Alumina Reinforcement of Different Volume Fraction on Wear Characteristics of AL 7075 Hybrid Composites Using Response Surface Methodology', 2016. DOI: https://doi.org/10.1590/1980-5373-MR-2022-0204
2. Gebre Fenta Aynalem, 'Processing Methods and Mechanical Properties of Aluminium Matrix Composites. Advances in Materials Science and Engineering: 2020
3. Madhan Prabhu Deva, A. Parthiban, B. Radha Krishnan, Adisu Haile, and Wubishet Degife 'Investigation of Wear Behaviour and Mechanical Properties of Titanium Diboride Reinforced AMMC Composites', 2022
4. John V. Foltz, Metallic Materials Branch, Naval Surface Warfare Center, White Oak Laboratory Charles M. Blackmon, Applied Materials Technology Branch, Naval Surface Warfare Center, Dahlgren Laboratory 'Metal-Matrix Composites', p903-912. DOI: 10.1361/asmhba0001101
5. Surappa MK. 'Aluminum matrix composites: Challenges and opportunities', Sādhanā. 2003;28 (Parts 1 & 2):319-334. DOI:10.1007/BF02717141
6. Dr. Mohan Kumar Pradhan, National Institute of Technology Raipur 'Hybrid Composites Processing, Characterization, and Applications Mechanical and wear properties of AL7075 Sic and graphite hybrid composite and optimization using utility additives method'.
7. Sevim Yolcular Karaoglu, Serdar Karaoglu, Imgesu Unal. Aerospace Industry and Aluminum Metal Matrix Composites. Volume 2, Issue 2, (2021), 73-81.
8. Francis Nturanabo, Leonard Masu and John Baptist Kirabira 'Novel Applications of Aluminium Metal Matrix Composites', DOI: http://dx.doi.org/10.5772/intechopen.86225
9. Srisaran Venkatachalam, S. Baskaran, R. S. Karrthik, Deepak B. Thimiri Govinda Raj, T. Ramesh Kumar, 'Titanium Diboride Reinforced Aluminum Composite as a Robust Material for Automobile Applications'
10. T. Donomoto, K. Funatani, N. Miura, and N. Miyake, 'Ceramic Fiber Reinforced Piston for High Performance Diesel Engines', SAE Paper 830252, Society of Automotive Engineers, 1984
11. Mahendra KV, Radhakrishna K. 'Characterization of stir cast Al-Cu- (fly ash + SiC) hybrid metal matrix composites. Journal of Composite Materials', 2010;44(8):989-1005

12. http://www.dviaviation.com/wear-friction-testing.html
13. Kumar S, Balasubramanian V. 'Developing a mathematical model to evaluate wear rate of AA7075/SiCp powder metallurgy composites', Wear. 2008; 264:1026-34.
14. S. Johny James, M. Ganesan, P. Santhamoorthy, P. Kuppan 'Development of hybrid aluminium metal matrix composite and study of property',
15. Alexander Tsouknidas, Luca Settineri, Pedro Arrazola, and Nikolaos Michailidis, 'Wear-Related Phenomena in Advanced Materials', 2011. Doi:10.1155/2011/842686
16. Wąsik A., Leszczyńska-Madej B., Madej M. Hot extruded Al5SiC-graphite composites: Effect of graphite on microstructure, flexural, compressive and wear resistance behavior. Journal of Manufacturing Processes. Volume 95, 2023, Pages 266-274
17. G. Pitchayyapillai, P. Seenikannan,K. Raja, and K. Chandrasekaran Al6061 Hybrid Metal Matrix Composite Reinforced with Alumina and Molybdenum Disulphide
18. S.W. Beckwith., Designing with composites: suggested 'best practices' rules. SAMPE J., 45 (1) (2009), p. 17
19. J. Jensin Joshua, P.S. Venkatanarayanan, Dalbir Singh., A literature review on composite materials filled with and without nanoparticles subjected to high/low velocity impact loads. Materials Today: Proceedings., 2020.
20. Osama Mohammed Elmardi Suleiman Khaya., Literature review on imperfection of composite laminated plates. Journal of Microscopy and Ultrastructure: 5 (2017); pp.119–122.
21. Saeed Asiri., Modeling and Analysis of Automotive Engine Crankshaft Made of Composite and Functionally Graded Materials. Application of Materials in Agricultural Engineering: volume (2022).
22. Kumar Sharma A., Bhandari R., Aherwar A., Rimašauskienė R., Matrix materials used in composites: A comprehensive study. Materials Today: Proceedings, Volume 21(3), 2020, Pages 1559-1562
23. Aydin F., Effect of solid waste materials on properties of magnesium matrix composites - A systematic review. Journal of Magnesium and Alloys:10(10), 2022; Pages 2673-2698.

24. Kogi Ibrahim T., Saleh Yawas D., Dan-asabe B., Abdulmumin Adebisi A., Taguchi optimization and modelling of stir casting process parameters on the percentage elongation of aluminium, pumice and carbonated coal composite. Scientific Reports: 13(1); 2023
25. Hussain, I. & Immanuel, R. J. Composite materials and its advancements for a cleaner engine of future. In Advances in Engine Tribology 169–191 (Springer, 2022)
26. S. Dhanasekar, Thayammal G.A., Lilly R.T, Kamesh V.V., Nageswara R.M, E. Shankar, Dharamvir, Suresh K.P., and Misganaw G.W. A Comprehensive Study of Ceramic Matrix Composites for Space Applications. Synthesis and Characterization of Advanced Green Materials for Automotive and Aerospace Applications: 2022
27. A. M. Nagaraja, S. Gururaja, and A. Udayakumar, "Tensile behavior of ceramic matrix minicomposites with engineered interphases fabricated by chemical vapor infiltration," Journal of the European Ceramic Society, vol. 42, no. 6, pp. 2659–2671, 2022.
28. Fakkir Mohamed M., Aluminum metal matrix composites and fabricating techniques - a review. 2020
29. Kolia D.K., Agnihotri G., Purohit R. Advanced Aluminum Matrix Composites: The Critical Need of Automotive and Aerospace Engineering Fields. Volume 2, Issues 4–5, 2015, Pages 3032-3041.
30. A.Thirumoorthy, T. V. Arjunan, K. L. Senthil Kumar, 2018, Latest Research Development in Aluminum Matrix with Particulate Reinforcement Composites – A Review, Materials Today: Proceedings 5, 1657–1665, 2018
31. B. Aldousiri, A. Shalwan and C. W. Chin., A Review on Tribological Behavior of Polymeric Composites and Future Reinforcements. Sustainable Composites: volume (2013).
32. Ravi Kumar, V Dileep B P and Vital H R, Tribological and Mechanical Characterization of Al-Ni-Sic Metal Matrix Composites, AIP Conference Proceedings, 1-6, (2017).
33. Jaswinder Singh, Amit Chauhan, Characterization of hybrid aluminum matrix composites for advanced applications – A review, Journal of Material Research Technology, 5(2), 159–169, (2016)
34. Kumar GV, Rao C, Selvaraj N. Mechanical and dry sliding wear behavior of Al7075 alloy-reinforced with SiC particles. J Compos Mater. 2012; 46:1201-9.

35. S. Pradeep Devaneyan, R. Ganesh and T. Senthilvelan. On the Mechanical Properties of Hybrid Aluminium 7075 Matrix Composite Material Reinforced with SiC and TiC Produced by Powder Metallurgy Method. Indian Journal of Materials Science: 2017

36. C. Velmurugan, R. Subramanian, S. Thirugnanam, B. Anandavel, (2012),"Investigation of friction and wear behavior of hybrid aluminium composites", Industrial Lubrication and Tribology, Vol. 64 Iss: 3 pp. 152 - 163

37. C.G. Levi, G.J. Abbaschian, and R. Mehrabian. Interface interactions during fabrication of aluminum alloy-alumina fiber composites. Metallurgical Transactions: volume 9, p697–711 (19780)

38. H. Fukunaga, S.G. Fishman. Preparation of intermetallic compound matrix composites by reaction squeeze casting. Journal of Materials Science Letters volume: 10, pages23–25 (1991) 1988.

39. Rawal S. Metal-matrix composites for space applications. Journal of Management. 2001;53(4): p14-17

40. Kurumlu D, Payton EJ, Young ML, Schöbel M, Requena G, Eggeler G. High-temperature strength and damage evolution in short fiber reinforced aluminum alloys studied by miniature creep testing and synchrotron microtomography. Acta Materialia. 2012;60(1): p67-78

41. Withers PJ. Metal matrix composite. In: Access Science. United Kingdom: McGraw-Hill Education; 2014. DOI: 10.1036/1097-8542.418600

42. Y. C. Lin, H. C. Li, S. S. Liou, and M. T. Shie, "Mechanism of plastic deformation of powder metallury metal matrix composites of Cu-Sn/Sic and 6061/SiC under compressive stress," *Materials Science and Engineering A*, vol. 373, no. 1-2, pp. 363–369, 2004.

43. L. Shi, C. Sun, P. Gao, F. Zhou, and W. Liu, "Mechanical properties and wear and corrosion resistance of electrodeposited Ni-Co/SiC nanocomposite coating," *Applied Surface Science*, vol. 252, no. 10, pp. 3591–3599, 2006.

44. M. Reihanian, S. R. Asadullahpour, S. Hajarpour, and K. Gheisari, "Application of neural network and genetic algorithm to powder metallurgy of pure iron," *Materials and Design*, vol. 32, no. 6, pp. 3183–3188, 2011.

45. S. C. Tjong and Z. Y. Ma, “High-temperature creep behaviour of powder-metallurgy aluminium composites reinforced with SiC particles of various sizes,” *Composites Science and Technology*, vol. 59, no. 7, pp. 1117–1125, 1999.
46. Himanshu K, Merb K.S, Kumar S. Mechanical and Tribological Behaviors of Stir Cast Aluminum Matrix Composites. Procedia Materials Science 6 (2014) P1951 – 1960
47. M. Karbalaei Akbari, O. Mirzaee, H.R. Baharvandi, Fabrication and study on mechanical properties and fracture behavior of nanometric Al2O3 particle reinforced A356 composites focusing on the parameters of vortex method, Mater. Des. 46 (2013) 199–205
48. Kumar L. Tee, L. Lu, M.O. Lai, 1999, Synthesis of in situ Al-TiB_2 composites using stir cast route, Composite Structures 47, 589-593.]
49. T.F. Stephenson, J.A.E. Bell, in: R.A.L. Drew, H. Mostaghaci (Eds.), “Development and Applications of Ceramics and New Metal Alloys”, CIM, Montreal, 1993, p. 51.
50. N. Radhika, R. Subramanian, S. Venkat Prasat, B. Anandavel. Dry sliding wear behavior of aluminum/alumina/ graphite hybrid metal matrix composites, Industrial Lubrication and Tribology 64 (6) (2012) 359–366
51. Aisha H. Al-Moubaraki and Hind H. Al-Rushud., The Red Sea as a Corrosive Environment: Corrosion Rates and Corrosion Mechanism of Aluminum Alloys 7075, 2024, and 6061. International Journal of Corrosion: 2018. doi.org/10.1155/2018/2381287
52. V. I. Matkovich, ‘Boron and Refractory Borides’, Springer Verlag, New York (1977)
53. Yadav R, Meena A, Lee S Y, and Park S J, Experimental tribological and mechanical behavior of aluminum alloy 6061 composites incorporated ceramic particulates using Taguchi analysis, Tribol Int 192 (2024) 109243
54. Ronald G. Munro ‘Material Properties of Titanium Diboride’, Res. Natl. Inst. Stand. Technol. 105, 709-720 (2000)
55. T. B. Gemechu, Characterization of false banana/Glass fiber reinforced hybrid composite materials for wind turbine blades under fatigue load. 2022
56. S. Angadi, P.R. Konka, S. Bhavanasi, C.R. Bandaru, B.G. Kumari, B. Divya, S. Lakhanpa. Impact of TiB_2 Particles on Improving Processing Parameters of TiB_2/Al Metal Matrix Composites. MATEC Web of Conferences 392, 01026(2024)

57. Y.S. Kwon, J.S. Kim, H.T. Kim, J.S. Moon, D.V. Dubina, O.I.Lomovsky, “In-situ Synthesis of Cu-TiB_2 Nanocomposite by MA/SPS,” Journal of Korean Powder Metallurgy Institute, Vol. 10, No. 6, 2003]

58. B. Gopalakrishnan, C. Rajaravi, G. Udhayakumar, P.R. Lakshminarayanan, M.S. Prabhu. Analysis of mechanical properties of cold extruded Al 6061 TiB2 MMCs and validated for finite element analysis. Materials Today, Volume 43, Part 2, 2021, Pages 1283-1292]

59. S. Yang, R. Zhang, H. Liu, J. Li, H. Yan. Effect of La on microstructure and corrosion behavior of 10%$TiB_{2(p)}$/Al–5%Cu composites. Journal of Materials Research and Technology. 9(4):7047-7058. DOI: 10.1016/j.jmrt.2020.05.025

60. A. Ramesh, J. N. Prakash, A. S. Shiva Shankare Gowda and Sonnappa Appaiah, (2009). “Comparison of the Mechanical Properties of AL6061/Albite and AL6061/Graphite Metal Matrix Composites”. Journal of Minerals & Materials Characterization & Engineering (JMMCE) Vol. 8, No.2, pp 93-106. [DOI: 10.4236/jmmce.2009.82009]

61. B. N. Dhanunjayarao, Usha Kiran Sanivada and Raul Fangueiro ‘Effect of graphite particulate on mechanical characterization of hybrid polymer composites’, 2017

62. K. Mu’azu, M. Z. Sirajo, Muhammad M. Aliyu, I. Y. Suleiman, A. T. Mohammed, Effect of Particulate Reinforcements at Different Loads on Wear Behavior of Aluminum Alloy Reinforced with Aquaculture Waste. Environ. Sci., 2022, 13(12), pp. 1384-1392.

63. P. Sharma, K. Paliwal, R. Kumar, S. Sharma, A study on wear behaviour of Al 6101 / graphite composites, J. Asian Ceram. Soc. 5 (1) (2017) 42–48

64. Ramanathan, A., Krishnan, P. K., & Muraliraja, R. (2019). A review on the production of metal matrix composites through stir casting – Furnace design, properties, challenges, and research opportunities. Journal of Manufacturing Processes, 42(December 2018), 213–245. https://doi.org/10.1016/j.jmapro.2019.04.017

65. K. L. Tee, L. Lu, and M. O. Lai, “Improvement in mechanical properties of in-situ Al-TiB2 composite by incorporation of carbon,” Materials Science and Engineering A: vol. 339, no. 1-2, pp. 227–231, 2003.

66. T. V. Christy, N. Murugan, and S. Kumar, "A comparative study on the microstructures and mechanical properties of Al 6061 Alloy and the MMC Al 6061/TiB2," Journal of Minerals & Materials Characterization & Engineering: vol. 9, no. 1, pp. 57–65, 2010
67. https://labtesting.com/services/materials-testing/metallurgical-testing/microhardness-testing/
68. M. Malaki, A. F. Tehrani, B. Niroumand, and M. Gupta, "Wettability in metal matrix composites," Metals (Basel)., vol. 11, no. 7, pp. 1–24, 2021, doi:10.3390/met11071034.
69. D. N. Lawate, S. S. Shinde, and T. S. Jagtap, "Study of Process Parameters in Stir Casting Method for Production of Particulate," Int. J. Innov. Eng. Res. Technol., vol. 3, no. 1, pp. 1–5, 2016,
70. N. K. Tefera, Fabrication and Investigation of the effect of Machining Parameters on the Performance of Machining Al-TiB2 Composites. P(22-24), 2023
71. Krishnan, P.K.; Arunachalam, R.; Husain, A.; Al-Maharbi, M. Studies on the Influence of Stirrer Blade Design on the Microstructure and Mechanical Properties of a Novel Aluminum Metal Matrix Composite. J. Manuf. Sci. Eng. 2021, 143, 021008.
72. Ager P, Iortsor A, Obotu GM. Behavior of Aluminum Alloy Castings under Different Pouring Temperatures and Speeds. Discovery, 2014, 22(74), 62-71.
73. https://vietnamcastiron.com/aluminum-casting-temperature/#the-effects-of-casting-shape-on-aluminum-pouring-speed.
74. N. B. Dhokey and K. K. Rane. Wear Behavior and Its Correlation with Mechanical Properties of TiB2 Reinforced Aluminium-Based Composites. Advances in Tribology: Volume 2011, doi:10.1155/2011/837469
75. https://caeonline.com/buy/scanning-electron-microscopes/jeol-jsm-840/9063336
76. M. Manoj, J. Suresh Kumar, V. Mugendiran. R. Jinu., Effect of TiB2 Particles on the Morphological, Mechanical and Corrosion Behavior of Al7075 Metal Matrix Composite Produced Using Stir Casting Process. International Journal of Metal casting: 16(5), 2021.
77. Hareesha G, Chikkanna N, S. Doddamani, A. S. Kallimani. EFFECT OF ADDITION OF SiC PARTICLES ON THE MICROSTRUCTURE AND HARDNESS OF Al-SiC COMPOSITE. Metall. Mater. Eng. Vol 27 (1) 2021 p. 49-56 DOI:10.30544/590
78. https://www.ist.fraunhofer.de/en/expertise/analytics-testing-technology/pin-on-disk.html

79. Standard Test Method for Wear Testing with a Pin-on-Disk Apparatus, Designation: G 99 – 95a, may 2000
80. A. L. Crăciun, C. Pinca-Bretotean, C. Birtok-Băneasă, and A. Josan, Composites materials for friction and braking application. Materials Science and Engineering 200 (2017) 012009 doi:10.1088/1757-899X/200/1/012009
81. A. Vedrtnam, A. Kumar Fabrication and wear characterization of silicon carbide and copper reinforced aluminium matrix composite. Mater Discov, 1 (2018), 10.1016/j.md.2018.01.002
82. Azad, A. Shunmuga Priyan, Investigations on Coefficient of Friction and Surface Roughness of AA6061+ B4C Composites Produced by Stir Casting Process, Journal of Materials Science & Surface Engineering 6 (2018) 779–782
83. Rang Chen, Akira lwabuchi, Tomoharu Shimizu, Hyung Seop Shin, Hidenobu Mifune, "The sliding wear resistance behavior of NiAI and SiC particles reinforced aluminum alloy matrix composites", Wear 213 (1997) 175-184
84. Y. Wang, W.M. Rainforth, H. Jones, M. Lieblich, "Dry wear behaviour and its relation to microstructure of novel 6092 aluminium alloy–Ni3Al powder metallurgy composite", Wear 251 (2001) 1421–1432
85. S.K. Chaudhury, A.K. Singh, C.S. Sivaramakrishnan, S.C. Panigrahi, "Wear and friction behavior of spray formed and stir cast Al–2Mg–11TiO2 composites", Wear 258 (2005) 759–767
86. K. Krishnamurthy, M. Ashebre, J. Venkatesh, B. Suresha Dry sliding wear behavior of aluminum 6063 composites reinforced with TiB2 particles. J Miner Mater Charact Eng, 5 (2017)
87. Prakash K. S., Thankachan T., & Radhakrishnan R. Parametric optimization of dry sliding wear loss of copper–MWCNT composites. Transactions of Nonferrous Metals Society of China (English Edition), 27(3), 627– 637. (2017) https://doi.org/10.1016/S1003-6326(17)60070-0
88. Ermergen T, Taylan F. Investigation of DOE model analyses for open atmosphere laser polishing of additively manufactured Ti-6Al-4V samples by using ANOVA. Optics & Laser Technology. Volume 168, January 2024. https://doi.org/10.1016/j.optlastec.2023.109832
89. Pathan F., Gurav H., and Gujrathi S. Optimization for Tribological Properties of Glass Fiber-Reinforced PTFE Composites with Grey Relational Analysis. Journal of Materials. Volume 2016, Article ID 8981746, 7 pages. http://dx.doi.org/10.1155/2016/8981746

90. Graton, L.C. and Fraser, H.J, 1935, Systematic Packing of Spheres: With Particular Relation to Porosity and Permeability, Journal of Geology, v. 43, no. 8, pt.1, p. 785-909.
91. C.S. Ramesh, S. Pramod, R. Keshavamurthy. A study on microstructure and mechanical properties of Al 6061–TiB2. Materials Science and Engineering. volume 528(12) p4125–4132, 2011. https://doi.org/10.1016/j.msea.2011.02.024
92. S. Sivananthan, K. Ravi, C. Samson Jerold Samuel, Effect of SiC particles reinforcement on mechanical properties of Al6061 alloy processed using stir casting route. Materials Today proc. 21(1) 2020 968-970
93. Jojith, R., & Radhika, N. (2019). Mechanical and tribological properties of LM13/TiO2/MoS2 hybrid metal matrix composite synthesized by stir casting. Particulate Science and Technology, 37(5), 566–578. https://doi.org/10.1080/02726351.2017.1407381
94. Archard, J.F. (1953) Contact and Rubbing of Flat Surfaces. Journal of Applied Physics, 24, 981-988. https://doi.org/10.1063/1.1721448
95. Mansor, M. R., Sapuan, S. M., Zainudin, E. S., Nuraini, A. A., & Hambali, A. (2013). Stiffness prediction of hybrid kenaf/glass fiber reinforced polypropylene composites using rule of mixtures (ROM) and rule of hybrid mixtures (RoHM). Journal of Polymer Materials, 30(3), 321-334
96. Ma, Z.Y., Liung, Y.N., Zhang, Y.Z., Lu, Y.X. and Bi, J. (1996), “Sliding wear behaviour of SiC particle reinforced Al 2024 alloy composites”, Materials Science Technology, Vol. 12, pp. 751-756
97. K.F. Kelton, A.L. Greer. Nucleation in Condensed Matter, in Pergamon Materials Series, Volume 15, 2010, Pages 461-510
98. H.Q.Wang, W.L.Suna, Y.Q.Xing. Microstructure Analysis on 6061 Aluminum Alloy after Casting and Diffuses Annealing Process. Physics Procedia 50 (2013) 68 – 75 doi: 10.1016/j.phpro.2013.11.013
99. Wagih, A., Abu-Oqail, A., & Fathy, A. (2019). Effect of GNPs content on thermal and mechanical properties of a novel hybrid Cu-Al2O3/GNPs coated Ag nanocomposite. Ceramics International, 45(1), p1115–1124. https://doi.org/10.1016/j.ceramint.2018.10.001

100. Pradhan, P., Nanda, B. P., & Satapathy, A. (2020). Polyester composites filled with walnut shell powder: Preparation and thermal characterization. Polymer Composites, 41(8), 3294–3308. https://doi.org/10.1002/pc.25620

101. Cole M.E., S.D. Stout, V.M. Dominguez, A.M. Agnew. Pore Extractor 2D: An ImageJ toolkit for quantifying cortical pore morphometry on histological bone images, with application to intraskeletal and regional patterning. 179(3) 2022. https://doi.org/10.1002/ajpa.24618

102. Manoj Kumar Gupta, Brijesh Gangil, Lalit Ranakoti 'Mechanical and Tribological Characterizations of Al/TiB2 composites',

103. Manohar, G., Maity, S. R., & Pandey, K. M. (2021). Microstructural and mechanical properties of microwave sintered AA7075/graphite/SiC hybrid composite fabricated by powder metallurgy techniques. Silicon, 1-11

104. Sharma P., Paliwala K, Kumar Garg R, Sharma S, Khanduja D. A study on wear behaviour of Al/6101/graphite composites. 2017 5(1). DOI:10.1016/j.jascer.2016.12.007

105. P. J. Ross: Taguchi Techniques for Quality Engineering, McGraw-Hill International Book Company, Ohio, USA (1996)

106. Subramanian R, Kannan G, Nanjappan N, Vijayan K. Analysis of temperature distribution in wire electrical discharge machine on hybrid Al-MMCs. Indian Journal of Engineering and Materials Sciences. 2018; 25:301-306

APPENDIX

APPENDIX I: Product quality certificate of Al6061.

明泰铝业产品质量证明书

MING TAI AL. PRODUCT QUALITY CERTIFICATE

订货单位 Customer		编号： Serial No：	MT20041174
产品名称 Product	批号 Lot No	合金状态 Alloy And Temper	规格（mm） Dimension
铝板/铝带	GFG2003M60188	6061 T6	10*2000*4000
技术标准 Technique Standard	GB/T 3880-2012	化学成分标准 Composition Standard	GB/T 3190-2008

化学成分 % Chemical Composition

元素 Element	Si	Fe	Cu	Mn	Mg	Cr	Zn	Na	Ti	Al
标准值 Standard Value	0.4-0.8	≤0.7	0.15-0.4	≤0.15	0.8-1.2	0.04-0.35	≤0.25	---	≤0.15	余量
实测值 Measured Value	0.625	0.498	0.256	0.109	1.068	0.116	0.115	0	0.026	97.15

力学性能 Mechanical Property

取样方法 Sampling Method	抗拉强度（MPa） Tensile Strength		屈服强度（MPa） Yield Strength		延伸率（%） Elongation	
	标准值 Standard Value	实测值 Measured Value	标准值 Standard Value	实测值 Measured Value	标准值 Standard Value	实测值 Measured Value
横向	≥290	323	≥240	276	≥9	14

杯凸 Cup Bulge	标准值 Standard Value	——	制耳率（%） Earing	标准值 Standard Value	——
	实测值 Measured Value	——		实测值 Measured Value	——

90° 折弯 90° bend	合格	其他 Others	合格
表面质量 Surface Control	合格	几何尺寸 Dimension Control	合格
综合判定 Overall Conlusion	合格		

填表人： [illegible] Inspector：　　审批人： [illegible] Approver：　　日期： 2020年06月02日 Date

技术质量处

河南明泰铝业股份有限公司

地址：河南省巩义市回郭镇新310国道清中村中段　　邮编：451283

电话：0371-67554998　67554521　　传真：0371-67554518

APPENDIX II: Ordering Reinforcement Materials Online.

APPENDIX III: Micro hardness test results for Sample 5.

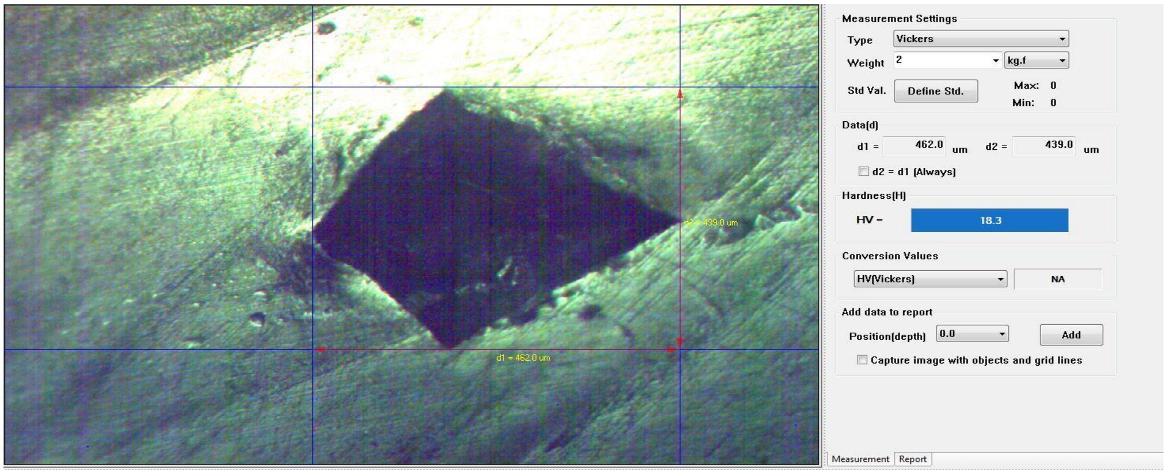

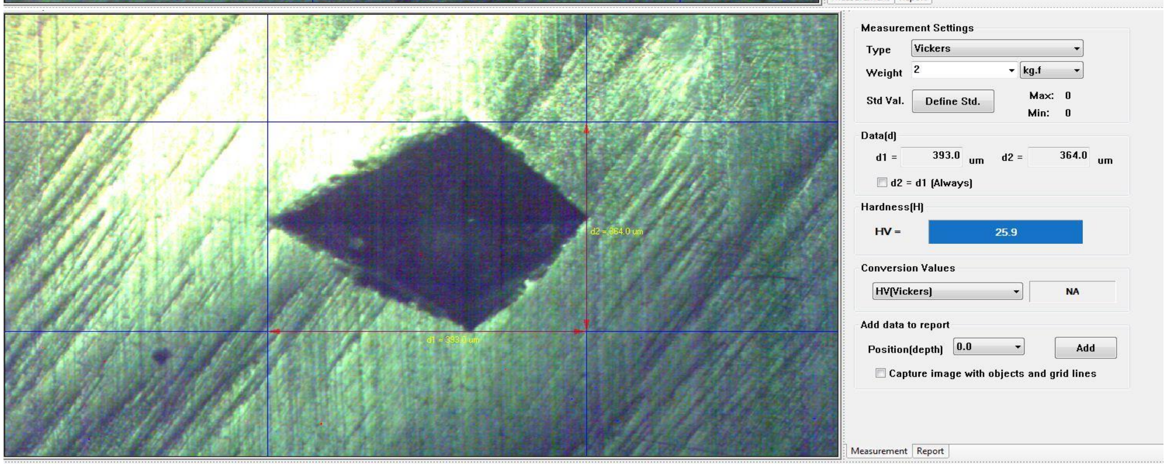

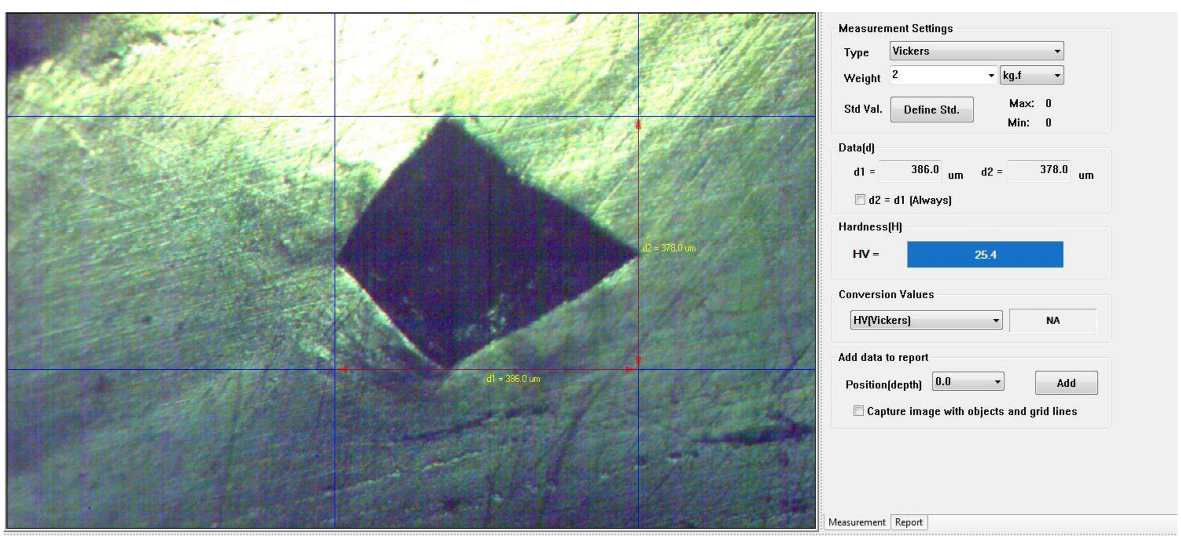

APPENDIX IV: Microhardness test specimens.

APPENDIX V: Taguchi Design for wear process optimization.

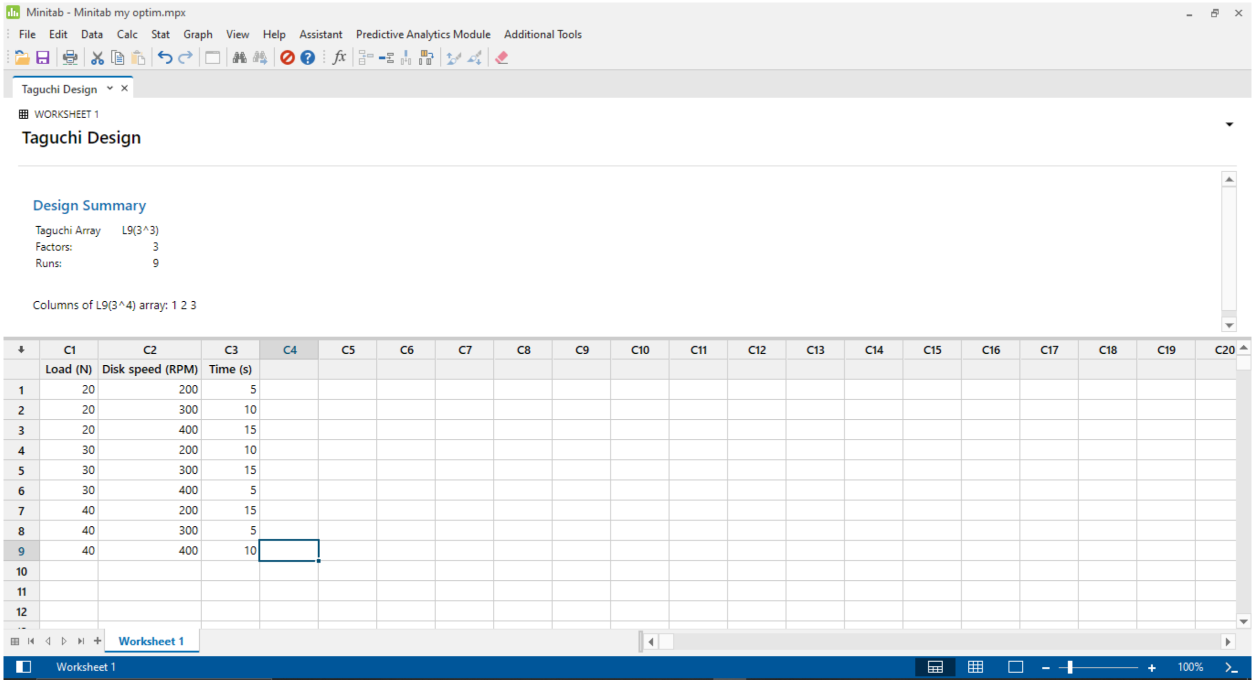

	C1 Load (N)	C2 Disk speed (RPM)	C3 Time (s)
1	20	200	5
2	20	300	10
3	20	400	15
4	30	200	10
5	30	300	15
6	30	400	5
7	40	200	15
8	40	300	5
9	40	400	10

APPENDIX VI: Taguchi analysis, ANOVA results, and regression equations from Minitab.

Response Table for Signal to Noise Ratios

Smaller is better

Level	Load (N)	Speed (RPM)	Time (Min)
1	15.19	24.06	17.89
2	30.29	22.45	22.93
3	16.66	15.63	21.32
Delta	15.10	8.43	5.05
Rank	1	2	3

Response Table for Means

Level	Load (N)	Speed (RPM)	Time (Min)
1	0.31077	0.06493	0.19213
2	0.03887	0.18043	0.07583
3	0.20307	0.30733	0.28473
Delta	0.27190	0.24240	0.20890
Rank	1	2	3

Regression Equation

COF = 0.4439 - 0.00100 Load (N) + 0.000250 Speed (RPM) - 0.00033 Time (Min)

Regression Equation

Wear 10-4(g/m) = -0.110 - 0.0054 Load (N) + 0.00121 Speed (RPM) + 0.0093 Time (Min)

APPENDIX VII: Confirmation test experimental result plots during the experiment.